FULL PAPER

A newly revised estimation of bulk densities and examination of the shape of individual Ryugu grains

Akiko Miyazaki[1*] , Toru Yada[1], Kasumi Yogata[1], Kentaro Hatakeda[1,2], Aiko Nakato[1,3], Masahiro Nishimura[1], Kana Nagashima[1], Kazuya Kumagai[1,2], Yuya Hitomi[1,2], Hiromichi Soejima[1,2], Rui Tahara[1], Rei Kanemaru[1], Arisa Nakano[1], Miwa Yoshitake[1], Ayako Iwamae[1], Shizuho Furuya[1], Akira Tsuchiyama[4,5,6], Shogo Tachibana[7], Tatsuhiro Michikami[8], Tatsuaki Okada[1], Masanao Abe[1,9] and Tomohiro Usui[1,10]

Abstract

The bulk density of grains from a celestial body is a fundamental property related to its composition and structure, contributing to the understanding of its evolutionary history. In this study, we provide the bulk density of 637 grains returned from the C-type near-Earth asteroid 162173 Ryugu. This is the largest number of grains to date for the curation activity, corresponding to 38 wt.% of the total returned samples (approximately 5.4 g). Although several densities of the Ryugu grains were reported, the volume estimation of some samples showed uncertainties. Therefore, we applied a new volume estimation model calibrated by X-ray micro-computed tomography (XCT) to the Ryugu grains to more accurately estimate their bulk density. The obtained average bulk density of 637 Ryugu grains was 1.79 ± 0.31 g/cm^3 (1σ variation) for weights of 0.5—100 mg (sub-mm —to 10 mm) irrespective of their 3D shapes characterized by three axial length ratios, considered to be a representative of the returned samples. The bulk density distributions of the grains in Chambers A and C were statistically distinguishable, with mean values of 1.81 ± 0.30 and 1.76 ± 0.33 g/cm^3 (1σ variations), respectively. Despite the small difference, bulk density may have differed by sampling site. The obtained average bulk density value of A + C samples was almost the same as that of 16 Ryugu grains estimated based on CT scanned data, and was consistent with the densities of CI chondrites (1.57–1.91 g/cm^3). The axial ratios of the grains in Chambers A and C were similar and those of the 724 returned samples and the flying particles ejected during the sampling operations were also similar, suggesting that relatively small Ryugu materials (mm—cm in size) are similar in shape. The minor difference between the Rygu grains and flying particles could be attributed to events such as scraping during sampling operations and transportation.

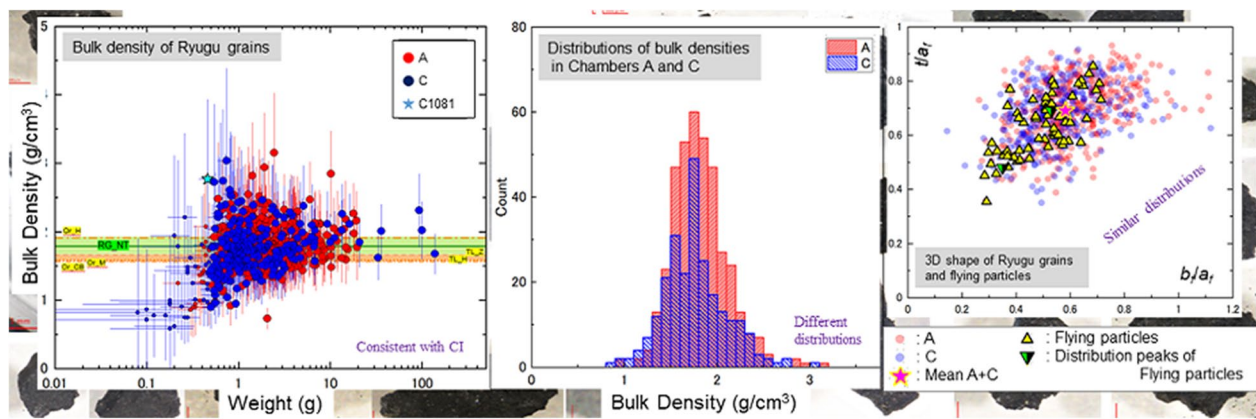**Keywords** Hayabusa2, Curation, Ryugu grains, Bulk density, 3D shapes

*Correspondence:
Akiko Miyazaki
miyazaki.akiko@jaxa.jp
Full list of author information is available at the end of the article

Miyazaki *et al. Earth, Planets and Space*   (2023) 75:171

Page 2 of 18

Graphical Abstract

Introduction

The Japan Aerospace Exploration Agency (JAXA) Hayabusa2 mission collected surface and sub-surface materials from the C-type near-Earth asteroid 162173 Ryugu and brought them back to Earth on December 6, 2020 (e.g., Tachibana et al. 2022). Ryugu samples were collected during two touch-down operations: the samples in Chamber A were collected and stored during the first touch-down operation (TD1) and the samples in Chambers C were collected and stored during the second touch-down operations (TD2) which was done near an artificial crater excavated by a small Carry-on Impactor (SCI) (Tachibana et al. 2022). Net weight of the returned samples was 5.424 ± 0.217 g (3.237 ± 0.002 g and 2.025 ± 0.003 g in Chambers A and C, respectively; Yada et al. 2022). Many preliminary descriptions and analyses on Ryugu samples, including size, weight, spectroscopic measurements, bulk compositions, mineralogy, chemistry, and isotopic composition, were conducted for nearly two years since the Ryugu samples were recovered from the sample containers (e.g., Yada et al. 2022; Pilorget et al. 2022; Nakamura et al. 2022a, b; Ito et al. 2022; Yokoyama et al 2022; Okazaki et al. 2022; Noguchi et al. 2023; Naraoka et al. 2023; Yabuta et al. 2023). Based on these results, the Ryugu samples were found to be materials similar to CI chondrites (e.g., Yada et al. 2022; Pilorget et al. 2022; Nakamura et al. 2022a, b; Yokoyama et al 2022).

Bulk density, defined by dividing the weight by the bulk volume including the pores, is a fundamental physical property closely related to the composition and structure of asteroid samples, and it affects the thermal properties of asteroids. Since Ryugu samples have a similar chemical composition as CI chondrites, it would be interesting to check if their densities are also similar. Several studies analyzed the bulk density of CI chondrites. The bulk density of one of CI chondrite, Orgueil meteorite, was reported to be around $1.57–1.91$ g/cm^3 (Consolmagno and Britt 1998; Britt and Consolmagno 2000; Hildebrand et al. 2006; Macke et al. 2011). Similar bulk density was reported for C2 ungrouped carbonaceous chondrite of Tagish Lake to be $1.57–1.71$ g/cm^3 (Zolensky et al. 2002; Hildebrand et al. 2006). The bulk densities of Orgueil (CI) and Tagish Lake (C2 ungrouped) meteorites were small among the other carbonaceous chondrites, i.e., $2–5$ g/cm^3 (Consolmagno and Britt 1998; Macke et al. 2011; Flynn et al. 2018). It was suggested that the small bulk density may be explained by many tiny fractures and voids present in those meteorites (e.g., Consolmagno and Britt 1998; Macke et al. 2011). The reported microporosity, defined as the volume ratio of voids within a grain, was as large as $23–43\%$ for these meteorites (Consolmagno and Britt 1998; Britt and Consolmagno 2000; Hildebrand et al. 2006; Macke et al. 2011). Those fractures and voids can be affected by weathering on Earth (e.g., Corrigan et al. 1997; Gounelle and Zolensky 2001) or by heating and fragmentation during entry into the Earth's atmosphere. Hence, it is not easy to ascertain the bulk density of CI chondrites unaffected by weathering or heating. Ryugu grains are pristine samples that have not been affected by weathering or heating, as the grains were protected within the heat-shield container during entry to Earth; they may represent pristine CI chondrites.

The bulk density of Ryugu samples was reported in several studies; however, some of them have uncertainties due to the volume estimation methods. The volume of the meteorite samples required to estimate their bulk

Miyazaki *et al. Earth, Planets and Space* (2023) 75:171

Page 3 of 18

densities was measured with the Archimedean method using 1 mm or less (-40 μm) sized glass beads (e.g., Consolmagno and Britt 1998; Britt and Consolmagno 2000; Hildebrand et al. 2006; Macke et al. 2011) or sieved quartz sand (500–700 μm in size; Zolensky et al. 2002). However, the Archimedean method is not ideal for measuring volume of Ryugu grains due to the small (several mm) and brittle nature of the grains; the grains would be contaminated with the glass beads themselves. Thus, we chose a different method without directly touching the sample to estimate the grain volume and then the bulk density of Ryugu grains, as described in earlier studies. Variations in the reported density values are listed in Table 1. Yada et al. (2022) estimated the first bulk density from 204 Ryugu grains to be 1.282 ± 0.231 g/cm^3 based on the analyzed grain weight and the volume estimated by adopting a spheroid model. Their estimated value was smaller than the one reported in other studies (Nakamura et al. 2022a, b; see Table 1). Nakamura et al. (2022a) used the three-dimensional (3D) model obtained by optical profilometry to estimate the grain volume, which resulted in the bulk density of 1.528 ± 0.242 g/cm^3 based on 16 Ryugu grains. Nakamura et al. (2022b) used X-ray micro-computed tomography (XCT) to image each grain and precisely estimated its volume, resulting in the grain densities ranging from 1.7 to 1.9 g/cm^3, with an average of 1.79 ± 0.08 g/cm^3, for 16 Ryugu grains. The low bulk density reported by Yada et al. (2022) may have been derived from an overestimation of the grain volume using a parameter that was not calibrated for the Ryugu sample in the spheroid model, where the volume was estimated from the 3D axial lengths. Therefore, in this study, we first established a new calibration method using a new correction factor for a more precise volume estimation model from 3D axial lengths. For this purpose, volumetric data points for 16 Ryugu grains obtained with XCT by Nakamura et al. (2022b) were used as references for the calibration. We then re-estimated the bulk density of 724 Ryugu grains, which corresponded to 40.3 wt.% of total returned samples (5424 mg). Based on the results, the average value and variation of the density of 724 grains were examined. As presented below, the Ryugu grains studied in this work varied in their 3D shapes, ranging from elongated to equant shapes. The shape difference may affect the volume estimation; thus, the relationships between the shape and the bulk density were also investigated.

The flying particles ejected from Ryugu during the touch-down operations were imaged using a small monitor camera head (CAM-H) of the Hayabusa2 spacecraft (Tachibana et al. 2022). We compared the 3D shapes of the retrieved Ryugu grains (sub-millimeter to 10 mm) with flying particles (centimeter in size). This provides a clue to the size and shape variations of the relatively small surface materials of Ryugu as well as to the bulk density and porosity of the surface materials.

Methods
Description procedures
The sample was processed by transferring grains from the container to the sapphire dishes, obtaining their optical images, and measuring their sizes and weights, following Yada et al. (2022, 2023) and we briefly describe the procedures presented below. All measurements were performed in a non-destructive and non-contaminated manner in a purified nitrogen environment in clean chambers (CCs), without exposure to the Earth's atmosphere. All the acquired data (optical images, sizes and weights) were archived in the Ryugu Sample Database (https://www.darts.isas.jaxa.jp/curation/hayabusa2/; Nishimura et al. 2023) and the analytical datasets including bulk density are summarized in Extended Table 1.

Grain transfer
Ryugu grains were hand-picked individually from the sample containers into individual sapphire dishes using vacuum tweezers. We selected 724 grains (420 from Chamber A and 304 from Chamber C) by December 2022 (see Table 2). Several grains from Chamber C

Table 1 Bulk densities of Ryugu grains and volume estimating methods

	Average bulk density[a] (g/cm^3)	Number of grains	Volume estimation method
Yada et al. (2022)	1.282 ± 0.231	204	Spheroid model of Eq. (1) based on a correction factor of 0.928 derived from Bagheri et al. (2015)
Nakamura et al. (2022a)	1.528 ± 0.242	16	3D model obtained by optical profilometry
Nakamura et al. (2022b)	1.79 ± 0.08	16	3D model obtained by X-ray computed tomography (XCT)
This work	1.79 ± 0.31	637	Spheroid model of Eq. (1) based on a correction factor of 0.860 ± 0.044, derived from Nakamura et al. (2022b) using XCT

[a] Density with 1σ variation

Miyazaki *et al. Earth, Planets and Space*   (2023) 75:171

Page 4 of 18

Table 2 Total numbers and weights of picked-up grains

Chamber	Picked-up grains			Samples in each chamber
	Number (n)	Total weight (mg)	Weight ratio[a] (wt.%)	Total weight (mg)
A	420	1166.5	36.0	3237
C	304	955.6	47.2	2025
C without C9000, C0001 and C0002	301	624.0	29.8	
A+C	724	2122.1	40.3	5262

[a] Weight ratio of the sum of picked up grains to the total weight of samples in each chamber

appear to be artificial objects (metal and polyimide tapes) that were used as spacecraft materials (Sawada et al. 2017). These grains were excluded from the subsequent analyses.

Image acquisition

Images of the grains were taken using a CMOS camera (Nikon DS-Fi3) mounted on the optical microscope (Nikon SMZ-1270i). The captured image was 1440×1024 pixels with the pixel size ranging from 0.34 to 3.85 µm depending on the magnification. For large grains out of the field of view, several images were taken and stitched together using an imaging software (NIS-Elements Ar, Nikon Instruments Inc.) to capture the entire grains. In-focus two-dimensional (2D) projected image was created by focusing every 140–400 µm depth of the grain depending on the magnification. The images captured at different depths were stacked together to create a single focused image using NIS-Elements Ar. Figure 1a shows the image after the stitching process of the largest Ryugu grain, C9000.

Size measurement

The major and minor dimensions of the projected image of a grain and its thickness were used to describe each grain in 3D. The in-focus 2D image was binarized using ImageJ software (https://imagej.net/ij/index.html) and the grain projection image was extracted as the Region of Interest (ROI). Two sets of major and minor dimensions were estimated for each ROI using ImageJ software. One is the major and minor diameters of the ellipses, a and b, which best fit the ROI (Fig. 1b: projection of C9000), and the other is the maximum and minimum Feret diameters, a_f and b_f, which correspond to the maximum and minimum caliper diameters of the ROI, respectively. As shown in Fig. 1c, the Feret diameters are not necessarily orthogonal. We measured the thickness of the grain t by focusing on the highest point of the sample and the surface of the sapphire dish representing the lowest point of the grain. By definition, t of the Ryugu grains is orthogonal to the projection plane. The depth of field of the microscope is 0.14–0.4 mm depending on the magnification. Among the three size measurements, the thickness represented a relatively large uncertainty. The uncertainty in thickness may be derived from a few factors: the depth of field of the microscope and operation-dependent measurement variation among the 10 measurers. The uncertainty in thickness measurement was on average nearly 20% of the measured value for 724 grains. The
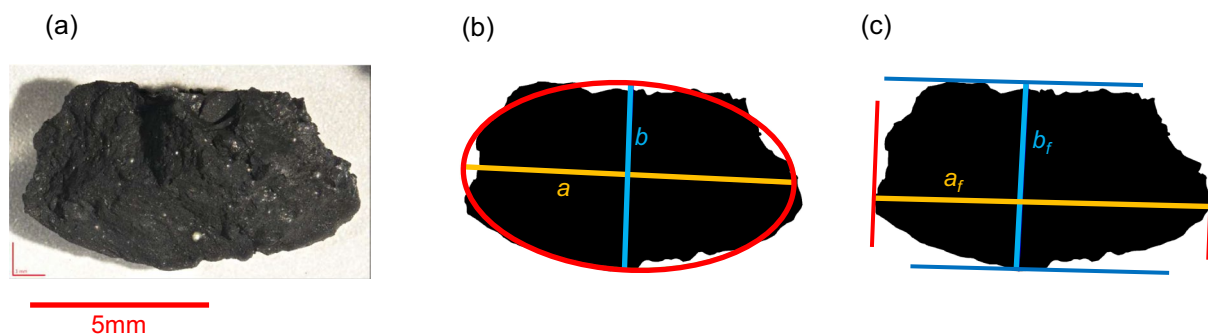

Fig. 1 Optical and projected images of the largest Ryugu grain, C9000. **a** Optical image after the composite process; 5×4 images were taken horizontally, and 11 layers of the images were stacked. **b** Major (a: orange line) and minor (b: blue line) diameters of the ellipse (red line) that best fit the projected area (ROI) of C9000. **c** Maximum (a_f: orange line) and minimum (b_f: blue line) Feret diameters of C9000. These two dimensions are not necessarily orthogonal. See text

uncertainties of two horizontal lengths (Δa and Δb or Δf_a and Δf_b) were indistinguishable and came from fluctuation in digitizing the extracted projection from the grain optical images, although the uncertainties were negligible (e.g., several tens of μm).

Weight measurement

The weights of the particles were measured using an electronic balance (Mettler-Toledo XP404s) in the CC under a metallic outer cover sealed with Viton. The static electricity generated during sample handling prevented the accurate measurement of the sample weight. Therefore, the main unit was grounded to avoid static electricity and a quartz glass windshield was lined with a stainless-steel mesh to cover the sample during the measurements (minimum scale value of 0.1 mg). The sample weight was obtained by subtracting the sapphire-dish weight from the total weight. The mean value of five replicate measurements was taken to reduce the weight measurement error. The weight measurement error of the 724 samples was in the range of 0.05–0.15 mg. When small particles or powders adhered to the grain surface or fell onto the dish, they were weighed together, which may have caused

an overestimation of the weights for the density estimation. Thirty four grains out of the 724 grains were omitted from the later density discussion because they were weighed together with relatively large sub-particles. The projected area of these sub-particles accounted for nearly 10% of the main grain in these 34 samples. However, in most cases, the weights of small particles or powders were negligible; therefore, they are included in the weight of the main grain. Thus, the remaining 690 grains were used to estimate the bulk density.

Shape characterization

3D axial ratios defined as b/a and t/a were used to characterize the shape of the Ryugu grains. Although the largest projected area of the grain was captured in the microscopic image taken from the top view when the grain was placed on a sapphire dish, grains with an axial ratio of $t > b$ were observed in some images (Fig. 2a). Therefore, we adopted a new dataset for the three-axial lengths (A, B, and T for $B/A > T/A$), where b and t were replaced if $t > b$ (i.e., $B = b$ and $T = t$ for $b > t$, $B = t$ and $T = b$ for $t > b$, and $A = a$). The dataset was used for shape characterization. We classified the Ryugu grain shapes
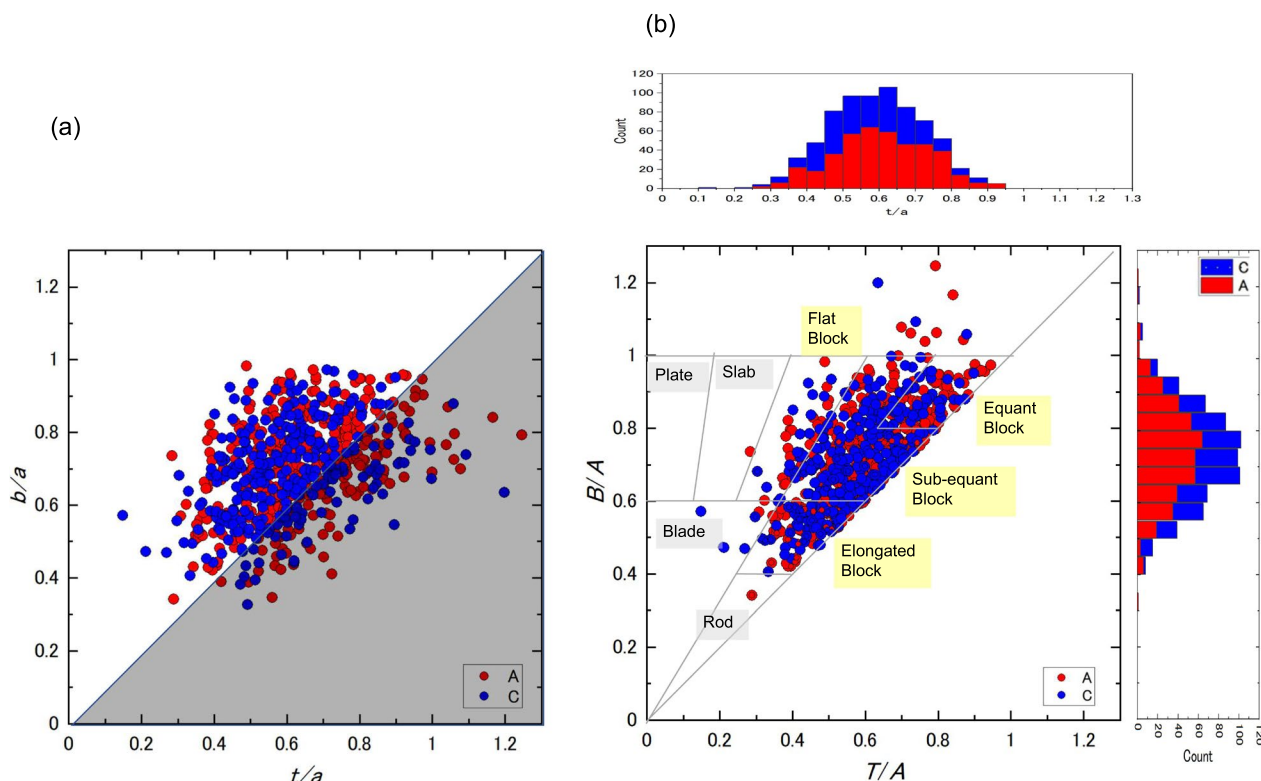

Fig. 2 Plot depicting the axial ratios of 724 Ryugu grains. **a** Distributions of *b/a* and *t/a* ratios of Ryugu grains. Grains plotted in shadowed area are the grains with *t/a > b/a*. **b** Distributions of *B/A* and *T/A* ratios of Ryugu grains; replot of **a**. Frequency distributions of the ratios are shown outside of the diagram. Mean *B/A* and *T/A* ratios are 0.73 and 0.59, respectively. The shape terminology is based on the classification described in Blott and Pye (2008). Typical grains corresponding to each classification are shown in Fig. 4

Miyazaki *et al. Earth, Planets and Space*   (2023) 75:171

Page 6 of 18

into eight categories based on the 3D axial ratios of T/A and B/A; "Rod", "Blade", "Plate", "Slab", "Flat Block". "Elongated Block", "Sub-equant Block", and "Equant Block" (Fig. 2(b)). The shape terminologies were based on the classification described by Blott and Pye (2008). Additionally, ten grains with $T/A > 1$, i.e., the thickness of each grain was larger than the maximum length of the projected image, were excluded from the current shape analyses. This reversion may be explained by the fact that tall grains remained standing due to electric static effects in the sapphire dish.

We adopted another set of 3D axial ratios using the Feret diameters (b_f/a_f and t/a_f), for comparison with flying particles ejected from Ryugu (Tachibana et al. 2022). They measured the three-axial lengths L, I, and S, instead of a, b, and t, where L and I are the caliper lengths of the maximum-area projection of each flying particle, respectively, and S is the minimum dimension of the minimum-area projection. As the largest-area projection of Ryugu grains was likely to be seen as a 2D image on a sapphire dish, we considered b_f/a_f of Ryugu grains and I/L of the flying particles to be comparable, and examined these data-sets. By definition, t of the Ryugu grains tends to be longer than S.

Density estimation

The bulk density of a grain was calculated from its weight and volume. The volume of Ryugu grains (V_g) was calculated using Eq. (1), as in Yada et al. (2022), although with a newly calibrated correction factor, k.

$$V_g = \frac{\pi}{6} \times \left(k \times D_g\right)^3. \tag{1}$$

Here, D_g, is the geometrically averaged 3D diameter of a grain,

$$D_g = \sqrt[3]{a * b * t}. \tag{2}$$

Individual correction factor (k) values for Ryugu grains, whose volumes (V_{XCT}) were measured individually using the XCT by Nakamura et al. (2022b), were calculated from Eq. (1) as follows:

$$k = \frac{1}{D_g} \times \sqrt[3]{\frac{6}{\pi} \times V_{XCT}} \tag{3}$$

Figure 3a shows the 16 individual k values versus D_g. The average k for 15 grains excluding one grain was 0.860 ± 0.044 (1σ variation), which was adopted for Eq. (1) in this study. Four candidates of k values were examined, of which the average value was considered most appropriate (see Appendix). Almost all data points, including the slightly large k value of C0002 (4.95 mm in size), were consistent with the average value of the range of uncertainty (Fig. 3a). The lowest data point of grain C0033 in Fig. 3a was excluded because the measured length of the sample differed significantly between Nakamura et al. (2022b) and this study. The smaller length of C0033 is probably explained by a potential size change, such as chipping, due to the brittle nature of Ryugu grains. The validity of the correction factor was assessed by comparing the individual grain volume (V_g) calculated from Eq. (1) by adopting $k=0.860$, with the volume (V_{XCT}) obtained by Nakamura et al. (2022b). A positive correlation between V_g and V_{XCT}, especially for small grains (Fig. 3b, c) indicated that the correction factor (k) used in this study was adequate for estimating the grain volume. The total volumes of the 15 grains in this work
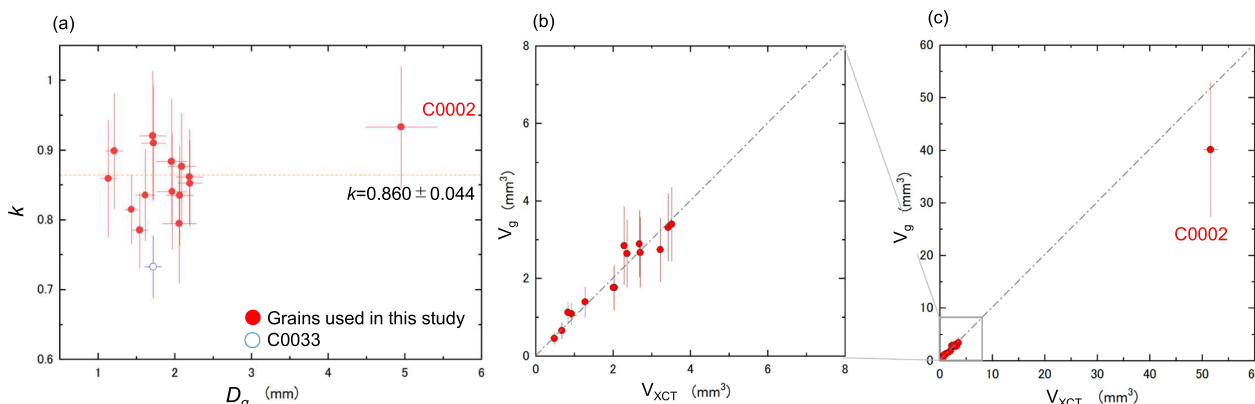

Fig. 3 Correction factor, k, and the correlation between V_{XCT} and V_g of Ryugu grains. **a** Correction factor, $k=0.860$, was determined from the geometrical mean of the individual k values of 15 grains. D_g represents geometrically averaged 3D diameter of the grains by Eq. (2). The data of C0033 are excluded because of the potential size change (e.g., chipping). **b** V_g of the 15 Ryugu grains were calculated using $k=0.860$ and compared to V_{XCT}, measured with XCT. **b** Is an enlarged plot of a part of **c**. Dotted line shows $V_g = V_{XCT}$

(69.38 ± 13.20 mm^3) and by XCT (80.04 ± 1.40 mm^3), in Nakamura et al. (2022b) agreed with each other within 1σ variation (see Table 4), which supported the validity of the correction factor.

The bulk density (ρ) of Ryugu grains was calculated by dividing the measured weight (M_g) by the volume (V_g) estimated from Eq. (1).

$$\rho = \frac{M_g}{V_g} \tag{4}$$

Kolmogorov–Smirnov test

We conducted a one-sample Kolmogorov–Smirnov (KS) static test to the obtained bulk density distribution and the axial ratios to verify whether the distributions were similar to normal distributions. Then we performed a two-sample KS static test to confirm whether the data sets of bulk density and axial ratios of the grains in Chambers A and C came from the same distribution. The KS statistics (values), the maximum difference between the two cumulative datasets, and *p*-values, the probability that two datasets have the same distribution, are summarized in Tables 5 and 6.

Results

Optical observations—overall descriptions

Here, we briefly describe the characteristics of Ryugu grains and introduce variations in their appearance and shape. For a detailed description and classification of the surface structures of the 205 Ryugu grains, refer to Nakato et al. (2023). Generally, the color and morphology
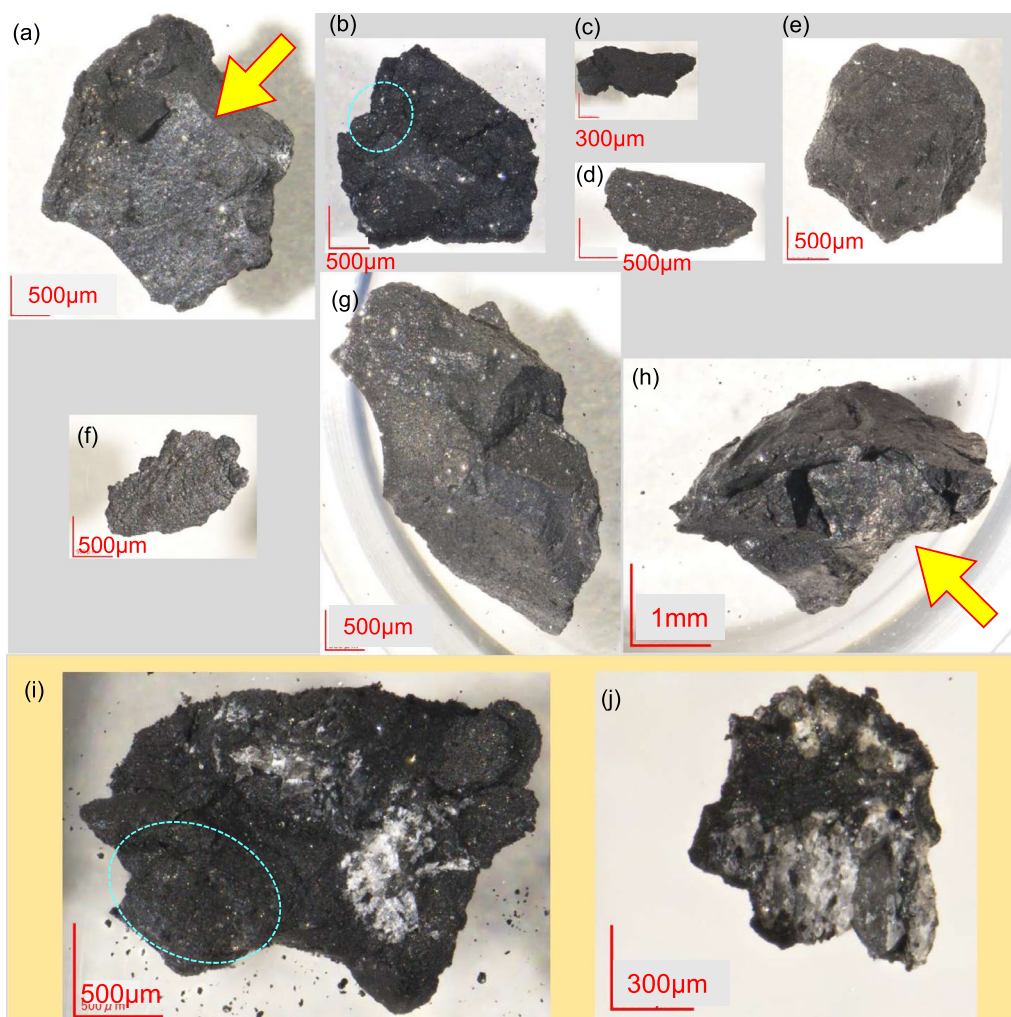

Fig. 4 Optical images of Ryugu grains with various shapes. **a** A0017 and **b** C0099; Flat Blocks, **c** A0195; Rod, **d** C0166; Blade, **e** A0114; Equant Block, **f** C0173; Slab, **g** A0016; Elongated Block, **h** A0004; Sub-equant Block. **i** C0041 and **j** C0181 are unique grains with large white/transparent materials. **i** and **j** are enlarged. Shape classification is based on Fig. 2b. The yellow arrows in **a** and **h** indicate glittering and/or glossy surfaces. Tiny bright materials are visible in the area enclosed by a dotted blue circle on grain (**b**) and (**i**)

Miyazaki *et al. Earth, Planets and Space*   (2023) 75:171

Page 8 of 18

were consistent with those reported in an earlier study (Nakato et al. 2023). Figure 4 shows typical grains of eight 3D shape groups (Fig. 4a–h) and unique grains (Fig. 4i, j). The Ryugu grains appeared black in color, with surface structures ranging from smooth (Fig. 4a) to rough (Fig. 4b). The 2D shapes were elongated (Fig. 4c, d) to equant (Fig. 4e) and the 3D shapes ranged from thin-plate (Fig. 4f) to thicker (Fig. 4g) shapes. Glittering and/or glossy appearances were often observed on the smooth surfaces of the grains (e.g., Fig. 4a, h), whereas grains with rough surfaces were often covered with tiny grains or powders (e.g., Fig. 4b, i). Large cracks are often observed, giving the grains an angular appearance (Fig. 4h). Several unique samples have been found, including large white materials (Fig. 4i, j). These grains, C0041 and C0181, belong to the "white group" of grains in the classification proposed by Nakato et al. (2023). Out of 724 grains, 32 "white group" grains were observed (17 and 15 from Chambers A and C, respectively). Part of C0041 was covered with white materials (crystals), whereas grain C0181 consisted almost exclusively of white/transparent crystals. The size of C0181 was as large as 1 mm, larger than the white material in C0041 (e.g., several hundreds

of µm). Nearly 80% of the Ryugu grains examined in this study contained tiny bright materials (Fig. 4b, i), most of which were determined to be Ca–Mg carbonate (dolomite; e.g., Nakato et al. 2023).

Bulk density

The bulk densities of individual Ryugu grains obtained in this work were plotted against their weights (Fig. 5). The obtained bulk densities greatly varied, ranging from 0.6 to 3.2 g/cm^3. Small grains had relatively low bulk densities (Fig. 5); out of 690 grains, 53 < 0.5 mg-sized grains had 1.29 ± 0.45 g/cm^3 (1σ variation) on average. As these small grains tended to have large volume estimation uncertainties ($\geq 40\%$), the bulk densities of ≥ 0.5 mg-sized grains were considered below. Although the variation in the bulk densities were large, ranging from 0.7 to 3.2 g/cm^3, the bulk densities of 637 Ryugu grains distributed around 1.8 g/cm^3. The frequency distributions of ≥ 0.5 mg-sized Ryugu grain bulk densities in Chambers A and C are separately plotted in Fig. 6. The 392 grains analyzed in Chamber A was 34 wt.% of the recovered A samples and the 245 grains analyzed in Chamber C was 44 wt.% of the recovered C samples (Table 3). The grains
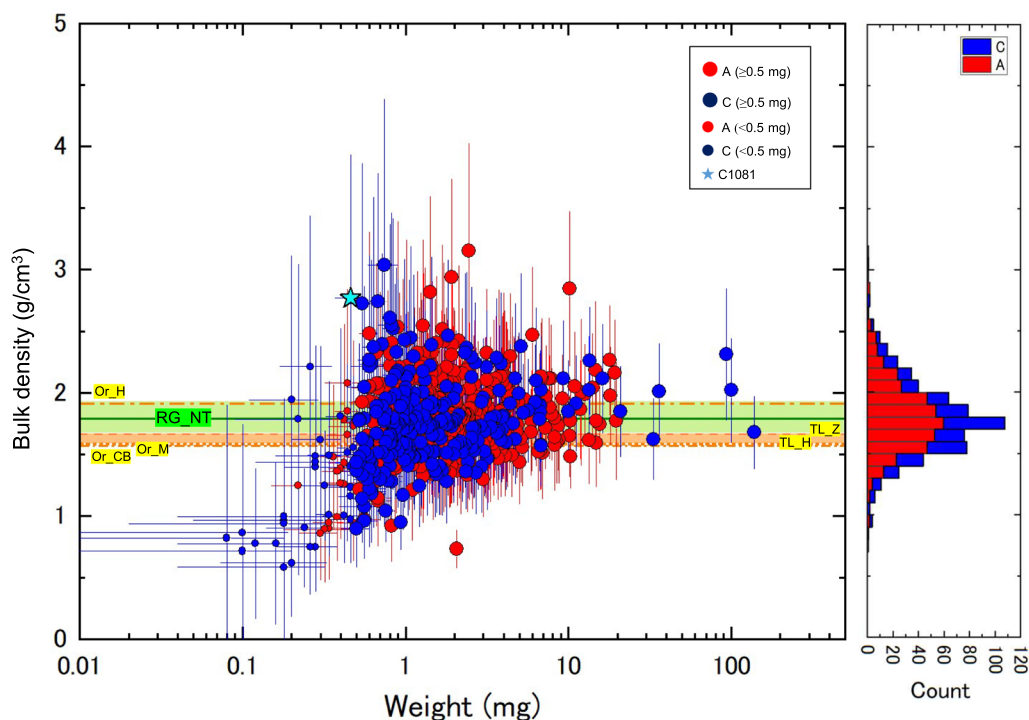

Fig. 5 Plot of the individual bulk density of Ryugu grains. The bulk density plotted against the weight. The frequency distribution of the density (A + C) is shown right of the scattered plot. Light green hatch labeled [RG_NT] shows the range of the bulk densities of 16 Ryugu grains by Nakamura et al. (2022b) and the green line represents the average value of 1.79 g/cm^3. The dashed orange lines and hatch show the bulk densities of Orgueil (Or) and Tagish Lake (TL) meteorites with labels consisting of the sample name ("Or" or "TL") and first letter of author's name: [Or_CB] (1.58 g/cm^3; Consolmagno and Britt 1998), [Or_H] (1.91 g/cm^3; Hildebrand et al. 2006), [Or_M] (1.57 g/cm^3, Macke et al. 2011), [TL_Z] (1.66 g/cm^3; Zolensky et al. 2002), and [TL_H] (1.58−1.71 g/cm^3; Hildebrand et al. 2006). The bulk density of C0181 is marked as a light blue star

Miyazaki *et al. Earth, Planets and Space*   (2023) 75:171
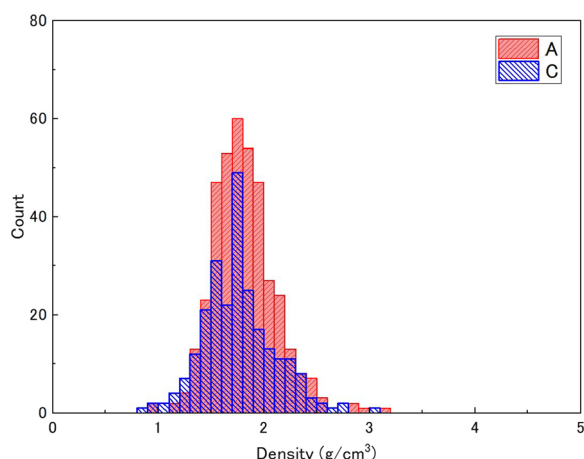
Page 9 of 18

Fig. 6 Distributions of the bulk density of Ryugu grains in each chamber. Frequency distributions of the bulk densities in Chambers A (red) and C (blue). They are plotted separate bar graphs

16 Ryugu grains estimated by Nakamura et al. (2022b) within 1σ variation. It was also in the range of the bulk densities of Orgueil meteorites, 1.57–1.91 g/cm^3 (Consolmagno and Britt 1998; Britt and Consolmagno 2000; Hildebrand et al. 2006; Macke et al. 2011) and rather higher than the bulk density of Tagish Lake meteorites, 1.57–1.71 g/cm^3 (Zolensky et al. 2002; Hildebrand et al. 2006). The bulk density of C0181 consisting almost exclusively of white crystals was 2.77 ± 1.16 g/cm^3, and is plotted in Fig. 5 for comparison despite the small grain weight (0.46 mg).

The bulk densities of the four major shapes ("Flat Blocks", "Elongated Blocks", "Sub-equant Blocks", and "Equant Blocks") were compared (Fig. 7). They shared similar values centering at 1.79 g/cm^3, indicating that the volume and thus the bulk density were not affected by the shape at least for these four forms.

in Chambers A and C were found to have nearly normal distributions based on the one-sample KS test, with average values of 1.81 ± 0.30 ($p = 0.14$) and 1.76 ± 0.33 g/cm^3 ($p = 0.12$; 1σ variations), respectively (see Table 5). Then, we performed the two-sample KS test to compare the bulk density distributions of the grains between Chambers A and C. The bulk density distributions of the grains in Chambers A and C were statistically distinguishable ($p = 0.04$), despite the difference in the average values being small. In Fig. 5, frequency distribution of the bulk density of the $637 \geq 0.5$ mg-sized Ryugu grains is shown on the right side of the scatter plot. Although the density data for all ≥ 0.5 mg-sized grains in Chambers A and C analyzed did not strictly follow a normal distribution, the data points appeared to be almost evenly distributed around the median or average value (Fig. 5). The total weight of 637 grains was 2002.6 mg, corresponding to 38.1 wt.% of the recovered A + C samples (Table 3); the average bulk density value can be considered to represent the entire returned sample.

The obtained individual and combined average bulk densities of the grains from Chambers A and C coincided with the average bulk density (1.79 ± 0.08 g/cm^3) of the
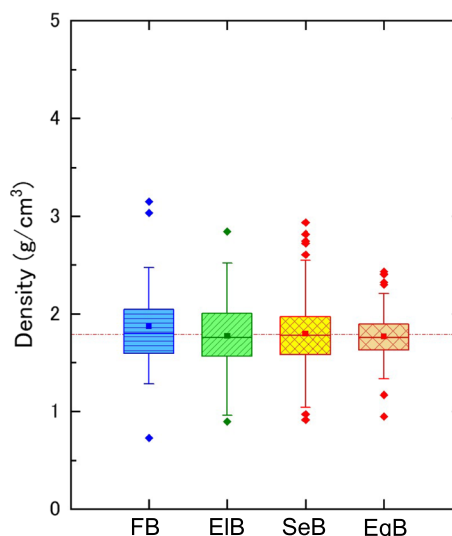

Fig. 7 The bulk density of Ryugu grains of four major shapes. Each box represents data points from the first to the third quartile and each bar represents the distribution of the data points; those beyond the bars are outliers. The grain shape classifications are FB: Flat Block, ElB: Elongated Block, SeB: Sub-equant Block and EqB: Equant Block, based on Fig. 2b. The dotted red line shows the average bulk density of the 637 Ryugu grains (1.79 g/cm^3)

Table 3 Bulk density of 637 Ryugu grains (≥ 0.5 mg)

	Number	Average bulk density[a] (g/cm^3)	Analyzed grains (mg)	Weight ratio[b] (wt.%)	Samples in each chamber (mg)
Chamber A	392	1.81 ± 0.30	1113.1	34.4	3237
Chamber C	245	1.76 ± 0.33	889.5	43.9	2025
Chamber A + C	637	1.79 ± 0.31	2002.6	38.1	5262

[a] Density with 1σ variation

[b] Weight ratio of the sum of analyzed grains to the total weight of samples in each chamber

Miyazaki *et al. Earth, Planets and Space* (2023) 75:171

Page 10 of 18

Weight and size distributions

The total weight of the 724 picked-up grains was 2122.1 mg (Chamber A: 1166.5 mg, and Chamber C: 955.6 mg), which corresponded to 40.3% of the total weight of the Ryugu samples in Chambers A and C (5262 mg) (Table 2). Chamber C contains several relatively heavy grains. C9000 was the heaviest (138.1 mg) and largest (10.38 mm) grain among the Ryugu samples. Two other extremely heavy and large grains observed were C0001 with 100.0 mg in weight and 7.36 mm in length, and C0002 with 93.5 mg in weight and 8.65 mm in length. The total weight proportion of picked-up grains from Chamber C decreased to 30 wt.% when these three grains were excluded (Table 2). The heaviest and largest grain in Chamber A was A0021 (25.8 mg and 5.13 mm). The small grains, mainly below 1 mm and/or sub-milligrams, are still being picked up and counted, and the data will be included in future analyses.

The cumulative weight and size distributions of Ryugu grains (Chambers A and C) are shown in Fig. 8. The log plot of the weight distribution is approximately linear for grains heavier than ~1 mg, and the log plot of the size (maximum Feret diameter) distribution also shows linearity larger than ~1.5 mm although these plots may show power-law distributions because the ranges of the weight and size are not wide. Assuming the power-law distributions for the weight and size of ≥ 1.0 mg and the ≥ 1.5 mm, the slopes are approximately -1.1 and -3.4, respectively, for total A+C grains. The ratio of the weight and size slopes is nearly 1:3, suggesting that grain weights are proportional to the cube of the major

diameters of the grain. This is consistent with the prediction that the bulk densities have similar value when grain are ≥ 1.0 mg.

Shape characterization

Ryugu grains ranging from long elongated to equant shapes in 2D were categorized into eight 3D shapes (Fig. 2b). Most common shapes observed in the Ryugu grains were "Elongated Block", "Sub-equant Block", and "Equant Block", followed by "Flat Block". A typical grain in the category of "Elongated Block" was represented by A0016 (Fig. 4g), "Sub-equant Block" by A0004 (Fig. 4h), "Equant Block" by A0114 (Fig. 4e) and "Flat Block" by A0017 (Fig. 4a) and by C0099 (Fig. 4b). The frequency distributions of B/A and T/A ratios are shown at the top and right sides of the frame of the T/A vs. B/A diagram (Fig. 2b). The average values of B/A and T/A ratios of the grains were 0.73 ± 0.13 and 0.59 ± 0.13, respectively.

We compared the shapes of the 724 Ryugu grains examined in this study with those of flying particles ejected from the Ryugu surface during touch down operations, as described by Tachibana et al. (2022). Figure 9 illustrates the plots of the axial ratios of the b_f/a_f and t/a_f of the Ryugu grains and the I/L and S/L of the centimeter-sized flying particles. The average b_f/a_f and t/a_f ratios of the grains in Chamber A were 0.70 ± 0.11 and 0.60 ± 0.14, respectively, and in Chamber C were 0.68 ± 0.11 and 0.56 ± 0.14, respectively. The result of the two-sample KS test suggested that the distributions of the t/a_f ratio of the grains in Chambers A and C were not the same ($p = 0.00$), while the b_f/a_f ratios were found to be similar ($p = 0.09$,
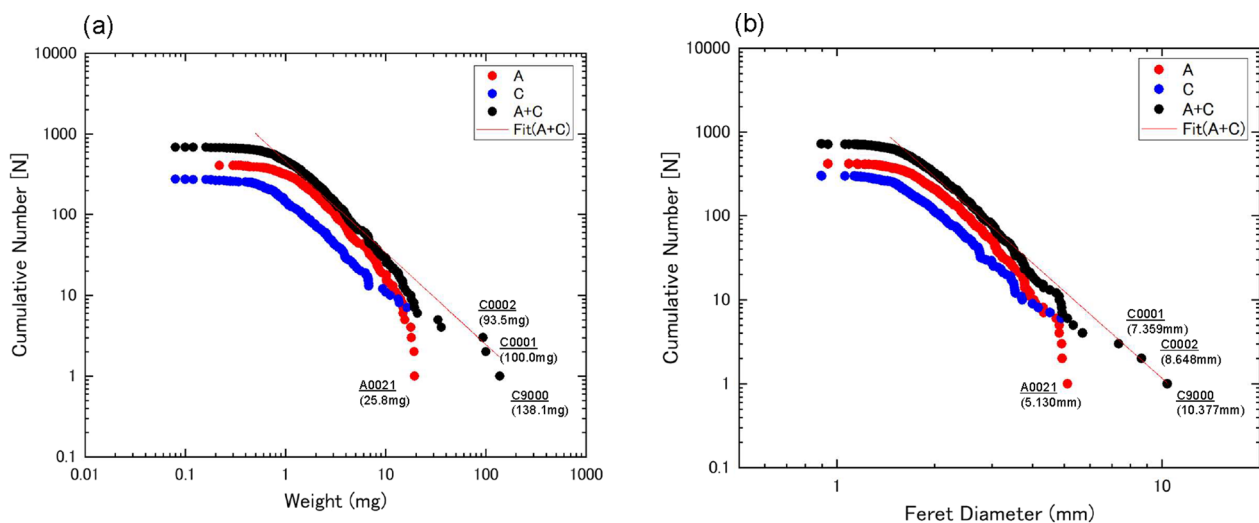

Fig. 8 Weight and size distributions of Ryugu grains. **a** Plot of cumulative distributions of weight and **b** size of Ryugu grains. Assuming the power law for the weight range heavier than 0.5 mg, the estimated power-index of total A+C grains is -1.1 (pink line). Whereas, assuming the power law for the size range larger than 1.5 mm, the estimated power-index of total A+C grains is -3.4 (pink line). The ID numbers, weights, and sizes of the four larger samples (a grain from Chamber A and three from Chamber C) are also noted in the figure
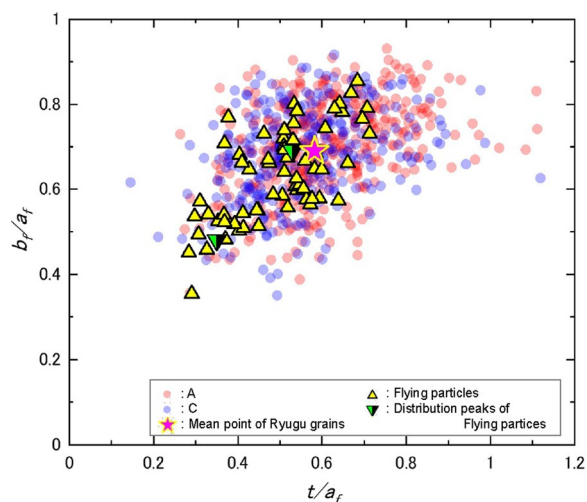
Miyazaki *et al. Earth, Planets and Space*   (2023) 75:171

Page 11 of 18

Fig. 9 Figure comparing 3D shape of Ryugu grains and flying particles. The shape data of flying particles were cited from Tachibana et al. (2022). Mean b_f/a_f and t/a_f ratios of 724 Ryugu grains (a pink star) are 0.69 and 0.58, respectively, which are close to one of bimodal distribution peaks of the flying particles (green triangles) of 0.69 and 0.53, respectively. Grains plotted $t/a_f > 1$ region are the grain with $t > a_f > b_f$

see Table 6). As shown in Fig. 9, b_f/a_f ($\sim I/L$) and t/a_f ($\sim S/L$) of the Ryugu grains and flying particles were scattered in nearly the same region, however, their distributions were not the same based on the two-sample KS test ($p = 0.00$ for both b_f/a_f ($\sim I/L$) and t/a_f ($\sim S/L$), respectively, see Table 6). The bimodal distribution was proposed for the flying particles by Tachibana et al. (2022), while it was not observed in this study. The mean b_f/a_f and t/a_f ratios of 0.69 and 0.58, respectively, were similar to one of bimodal distribution peaks of the flying particles whose I/L ($\sim b_f/a_f$) and S/L ($\sim t/a_f$) were 0.69 and 0.53, respectively (Tachibana et al. 2022).

Discussions and implications
Bulk density of Ryugu grains
As previously mentioned, the obtained bulk densities of ≥ 0.5 mg-sized grains ranged from 0.7 to 3.2 g/cm^3 (Fig. 5). No special surface characteristics were found among the grains with high bulk densities (≥ 2.8 g/cm^3) nor those with low densities (≤ 1.0 g/cm^3). The cracking and surface features of the grains had no apparent differences based on optical microscopic observations. The large variation in the obtained bulk densities was mainly due to the uncertainty in volume estimation of each grain. Uncertainties originating from the correction factor k in Eq. (1) and from the thickness measurement were significant. Therefore, the spread of the bulk densities in Fig. 5 does not represent the real variation of the bulk densities of individual Ryugu grains; it would be in

a narrower range. The volume estimation model does not depend on shape because the bulk densities were shape-independent for at least four forms; flat, elongated, sub-equant, and equant blocks (Fig. 7). The fact that the bulk densities of the grains in Chambers A and C were statistically different (see, "Bulk density" section) suggested the potential variation in the bulk density of returned Ryugu samples, 1.76–1.81 g/cm^3. The similar density variation ranging from 1.7 to 1.9 g/cm^3 were reported for 1–8 mm-sized Ryugu grains by Nakamura et al. (2022b). The variation in bulk density was expected to be at least 1.7 to 1.9 g/cm^3 or wider.

Larger bulk density of the grains in Chamber A than in Chamber C was also reported by Nakamura et al. (2022a) with relatively higher amount of voids of the grains in Chamber C than in Chamber A, but this trend was not observed by Nakamura et al. (2022b). The difference in bulk density of the grains between Chambers A and C may be derived from the (1) different degree of space weathering, or (2) impact of SCI or (3) local heterogeneity of the sampling sites. As for the degree of space weathering, Yada et al. (2022) predicted that the samples in Chamber A, collected during the TD1 operation, represented the surface materials of Ryugu, while some of the samples in Chamber C, collected during the TD2 operation, represented subsurface materials excavated by the impact experiments. The surface materials were considered to experience long-term exposure to space and had been significantly affected by weathering. Grains in Chamber A having density values larger than in Chamber C was consistent with the hypothesis that space weathering caused surface amorphization and partial melting of the grains suggested by Noguchi et al. (2023). However, such weathered layers were reported to be only < 100 nm in thickness (Noguchi et al. 2023). Thus, space weathering was unlikely to have contributed to the bulk density; the reported weathered layers may be too thin to explain the difference in the bulk densities of the grains between Chambers A and C, 1.80 and 1.76 g/cm^3, respectively. Therefore, solar radiation or space weathering might have little influence on the bulk density. As for the impact of SCI, many cratering ejecta had been collected during the TD2 operation and stored in Chamber C (Tachibana et al. 2022). The impact of the cratering operation with SCI may have caused the increased degree of fracturing in ejected grains or particles, possibly explaining the smaller bulk density of the grains in Chamber C compared with Chamber A. As for the local heterogeneity in the mineral mode, slight differences in mineral modes present in the Ryugu samples may be reflected as differences in bulk density. Further studies are required to clarify what may have caused these differences between the chambers.

Miyazaki *et al. Earth, Planets and Space*   (2023) 75:171

Page 12 of 18

Although the difference in the average bulk density of the grains between Chambers A and C was within 1σ variation and the spread in the individual bulk densities of the grains were present, a representative value of the returned samples can be determined by obtaining the average of all data. The ratio of the slope of cumulative distribution of weight to size of Ryugu grains, approximately 1:3 (Fig. 8), in the range of ≥ 0.5 mg and ≥ 1.5 mm, suggests that the bulk density of A + C grains does not have large range; the density is not largely dependent on the weight and size. Therefore, we propose that the average bulk density, 1.79 ± 0.31 g/cm^3 (1σ variation) for 637 Ryugu grains obtained in this work—using the largest number of Ryugu samples examined so far—represents the bulk density of Ryugu returned samples.

Consistency of the average bulk density values between the 637 Ryugu grains (≥ 0.5 mg or ≥ 1.5 mm) in this work and 16 Ryugu grains (1–8 mm in size) by Nakamura et al. (2022b) supports that the average bulk density of 1.79 g/cm^3 obtained in this work represents the Ryugu returned samples. Nakamura et al. (2022b) proposed physical and chemical models of the formation and evolution of asteroid Ryugu using their bulk density data. The results also showed that no revision is required for their model. The weight of 16 Ryugu grains analyzed by Nakamura et al. (2022b) (145.2 mg) corresponded to 2.8 wt.% of total Ryugu samples. This indicates that the Ryugu sample is homogeneous if at least 150 mg is considered. Assuming that the bulk density of the Ryugu grains obtained in this work was 1.79 g/cm^3, 150 mg of the Ryugu sample is equivalent to 4.4 mm in cubic size. The low bulk density reported by Yada et al. (2022), the first bulk density measurement from 204 Ryugu grains (1.282 ± 0.231 g/cm^3), was derived by overestimating the grain volume as follows: They used the volume estimation model based on Eq. (1), but adopted the correction factor, k, of 0.928 reported in Bagheri et al. (2015) that was calibrated for different materials (terrestrial volcanic clasts) and different size range (0.1 to 36 mm). A much more inadequate reason for the inappropriate value of k for the volume estimation of Ryugu grains is that the methods used to obtain the 3D axial lengths were different. We confirmed that the un-calibrated method of Yada et al. (2022) resulted in a lower density value. Another bulk density estimation, 1.528 ± 0.241 g/cm^3 based on 16 Ryugu grains, was reported by Nakamura et al. (2022a) who used the 3D model obtained by optical profilometry to estimate the grain volume. The bulk density estimated by Nakamura et al. (2022a) was lower than 1.79 g/cm^3 obtained in this work. Their approach tends to overestimate or underestimate the grain volumes due to the irregularity of the optically shaded area of the grains.

The appearance of the grains under microscopic observations, i.e., their surface characteristics classified by Nakato et al. (2023), seemed to have little effect on the bulk density. The only exception was C0181, which consisted almost exclusively of white/transparent crystals and had a relatively high bulk density of 2.77 ± 1.16 g/cm^3 (Fig. 5) despite its cracks or cleavages. C0181, together with C0041, considered "white group" grains (Nakato et al. 2023). Based on the results of the field emission-scanning electron microscopy/energy dispersive X-ray spectroscopy (FE-SEM-EDS) and near-infrared hyperspectral microscope MicrOmega, the white material in sample C0041 was found to be Mg-Fe carbonate (breunnerite; Nakato et al. 2023; Loizeau et al. 2023), while grain C0181 was found to contain complex carbonate-rich structures of crystals through MicrOmega analysis (Loizeau et al. 2023). Whether the carbonates in C0181 are dolomites (Ca-Mg carbonate, 2.84 g/cm^3; Mindat.org (2023)), which are frequently found in Ryugu samples, or breunnerites [Fe-bearing magnesite, > 2.98 g/cm^3; Mindat.org (2023)], which were found as relatively large carbonate minerals (Nakato et al. 2023; Loizeau et al. 2023), it must be contribute to the higher bulk density than other Ryugu grains.

Comparison with meteorites

The fact that the bulk densities of Ryugu grains are within the range of those of CI Orgueil meteorites (see, "Weight and size distributions" section) is consistent with Ryugu samples being analogues to CI chondrites. However, we need to consider the cause of the bulk density variation in CI (Orgueil) chondrites when further comparing the bulk density between Ryugu and meteorites. There are several possible factors for the density variation: the heterogeneity in the petrological features of the chondrite samples, the volume estimation method, and the weathering process on Earth. The CI chondrites are not always uniform. If the heterogeneity in the petrological features (i.e., mineral abundance) between the CI chondrites and Ryugu grains is similar to each other, then the heterogeneity is canceled out by measuring relatively large quantities. Generally, 10–100 g of the sample was used to measure the density of the CI chondrites. Thus, the first factor was not an issue. In the volume estimation method, the spherical beads or quartz sand used to measure the sample volume were assumed to behave as incompressible fluids of constant density. However, real beads and sand do not behave ideally; the packing efficiency of glass beads and quartz sand can be affected by the environment. Recently, the bulk densities of two CI chondrites, Orgueil and Ivuna, were revealed to be 1.61 ± 0.01 g/cm^3 and 1.95 ± 0.01 g/cm^3, respectively, by measuring their volume using a laser scanning system (Macke, personal

Miyazaki *et al. Earth, Planets and Space*   (2023) 75:171

Page 13 of 18

communication). Since the bulk densities estimated by a laser scanning method showed similar variation to that obtained by the conventional method, it is more reasonable to assume that variation in the bulk density of individual meteorites exists than to assume the presence of significant errors in the Archimedean volumetric method. Regarding the third factor, weathering derived sulfates or ferrihydrites were observed in CI chondrites by several studies (e.g., Corrigan et al. 1997; Gounelle and Zolensky 2001) but they are known to be absent in Ryugu samples (e.g., Yokoyama et al. 2022). The CI chondrites might have undergone oxidation and aqueous alteration during their formation. This makes it difficult to estimate the extent to which weathering products fill the voids. Weathered or altered structure of CI chondrites is complex and its effect on the bulk density remains unclear. Due to the last factor, comparing the bulk densities of Ryugu grains and CI chondrites is limited.

Porosity estimations
Many small voids or fractures as small as a few micrometers and as long as several hundred micrometers were observed in Ryugu grains (e.g., Nakamura et al. 2022a, b). As the bulk density is determined from the weight and overall volume, including voids or cracks, it is significantly affected by the voids in a sample, i.e., the porosity. The microporosity of the Ryugu grains is defined as 1 minus the ratio of the bulk density obtained in this work to the average grain density of the Ryugu samples, which is the net density, excluding voids. Due to the difficulty in determining accurate grain densities for Ryugu samples, only one data point has been reported for Ryugu grains to date. Nakamura et al. (2022a) estimated the grain density of 2.59 ± 0.06 g/cm^3 (average of 16 Ryugu grains) based on the modal abundance of minerals in the Ryugu grains and the theoretical mineral densities. The microporosity estimated using the grain density of Ryugu sample, 2.59 ± 0.06 g/cm^3, was 30.9% if we used the present value of the bulk density. However, the estimated grain density may not be accurate because the reported modal abundances of minerals in Ryugu grains vary among grains (e.g., Nakamura et al. 2022a, b; Ito et al. 2022; Yokoyama et al. 2022). The microporosity estimated by adopting the grain density of Orgueil meteorite, 2.42–2.50 g/cm^3 (Consolmagno and Britt 1998; Hildebrand et al. 2006; Macke et al. 2011), was 26.0–28.4%. The grain density of Orgueil meteorite can also be affected by weathering on Earth; hence, the obtained values should be interpreted carefully. Although there was uncertainty in the estimated microporosity value of Ryugu samples (30.9% and 26.0–28.4%), the microporosity of Ryugu grains could be 26–31%, which may be in the range of the data for Orgueil meteorites, 23–35% (Consolmagno and Britt 1998;

Hildebrand et al. 2006; Macke et al. 2011) and slightly smaller than the latest value of $33.8 \pm 0.5\%$ (Macke, personal communication). Since the porosity of CI chondrite could be affected by the formation of altered materials, such as sulfate, inside the voids or cracks during weathering on Earth (Gounelle and Zolensky 2001), comparing the porosity of Ryugu grains and CI chondrites is limited.

Microporosity of the boulders and surface materials on Ryugu was estimated to be 30–50% based both on the remote sensing observations using the Thermal Infrared Imager (TIR) (Okada et al. 2019) and on on-site thermal measurements with a radiometer (MARA) on Mobile Asteroid Surface Scout (MASCOT) (Grott et al. 2019). The estimated value of microporosity in this study was close to the lowest value of microporosity for the average Ryugu boulders. The relatively higher porosity values of the boulders suggest that they were more porous than the Ryugu grains in this study. This may be due to the large size of the cracks (as large as the Ryugu grains examined in this study: 1–100 mm in size).

3D shape of Ryugu grains
The axial ratio of t/a_f had different distributions between the grains in Chamber A and C, while b_f/a_f had similar distributions based on the two-sample KS test. Uncertainty of b_f/a_f ratios were small because b_f and a_f were obtained from the same method. In contrast, t/a_f ratios may have large uncertainties because of the measurement method described in "Size measurement" section. Although the t/a_f distributions between the grains in Chambers A and C could be different, as similarly observed in the bulk density differences between Chambers A and C, further detailed studies are required.

The Ryugu grain samples at the curation facilities had a peak in the axial ratios of b_f/a_f and t/a_f close to one of the higher bimodal distribution peaks of the flying particles (Fig. 9; see "Bulk density" section); i.e., Ryugu grains appeared to have relatively higher b_f/a_f and t/a_f ratios than the I/L and S/L ratios of the flying particles, respectively. By definition, t is longer than S, which may explain the higher t/a_f ratios of Ryugu grains compared to S/L of flying particles. However, the reason for the high b_f/a_f ratio remains unclear when calculating a_f and b_f. The higher b_f/a_f ratio of Ryugu grains compared to flying particles suggests that most Ryugu grains were equant-shaped, based on 2D images. It is expected that the Ryugu grains were scraped mechanically in the container when the grains were collected and re-entered into the atmosphere of the Earth, which may have contributed to the lack of smaller I/L and S/L peaks in the bimodal distribution of Ryugu grains in this study, unlike flying particles (Tachibana et al. 2022). Even taking into account the effects described above, we consider that Ryugu grains

Miyazaki *et al. Earth, Planets and Space*   (2023) 75:171

Page 14 of 18

and flying particles have approximately the same shape, i.e., the millimeter- to centimeter-sized Ryugu materials have a uniform shape.

We need to consider what the mean axial ratio of $B/A = 0.72$ and $T/A = 0.59$ represents. The average axial ratios of b/a and t/a of the Ryugu boulders of > 5 cm were 0.71 and 0.44, respectively, and the shape of the Ryugu boulders was suggested to be similar to the laboratory impact fragments (Michikami et al. 2019). Here, a, b and c are the maximum dimensions of the boulders in three mutually orthogonal planes ($a \geq b \geq c$). Therefore, it is not straightforward to compare between the impact fragments the b/a and c/a and B/A and T/A. Nevertheless, the axial ratios of the Ryugu grains in this study did not seem to be significantly different from those of the Ryugu boulders, and the former could be more rod-like than the latter. However, detailed shape analysis is required for a rigorous comparison.

Summary

In this study, 724 Ryugu grains corresponding to 40.3 wt.% of the total returned samples—the largest sample size ever studied—to estimate their bulk densities using more reliable calibration method for estimating the grain volumes.

- Among 724 grains, the bulk densities of individual 637 Ryugu grains were estimated as 1.79 ± 0.31 g/cm^3 (1σ variation) for weights of 0.5–100 mg—we considered to be the representative of the sample returned from asteroid Ryugu. The obtained bulk densities were irrespective of their 3D shape. Consistence of the average bulk density between this work and that obtained using XCT method for 16 Ryugu grains supports the representativeness of the average bulk density of 1.79 g/cm^3.
- The bulk densities of the 392 grains in Chamber A and 245 grains in Chamber C followed separate distributions and exhibited average values of 1.81 ± 0.30 and 1.76 ± 0.33 g/cm^3 (1σ variation), respectively. Although the difference was small, the results suggested that their bulk densities may have varied by sampling site.
- The average bulk density of Ryugu grains in the range of 1.57–1.91 g/cm^3 reported for Orgueil CI chondrites appears to support that Ryugu samples are similar to CI chondrites.
- Microporosity of the examined Ryugu grains was roughly estimated to be 26–31%, which is slightly higher than the latest data for the Orgueil CI chon-

drite and is close to the lowest value for the average Ryugu boulders.
- The weight and size distributions show approximately linear distributions (≥ 1.0 mg and ≥ 1.5 mm). Assuming that the distributions follow the power law, the ratio of the slopes (weight-to-size distributions) is approximately 1:3, suggesting that the bulk densities of the Ryugu grains take approximately the same value in this range.
- The axial ratios of b_f/a_f and t/a_f of Ryugu grains showed similar distribution to flying particles ejected from the Ryugu surface during sampling operations. Millimeter- to centimeter-sized Ryugu grains and pebbles may have a nearly uniform shape despite the returned sample show some shape deviation due to the mechanical scrape in the container.

In this study, we reported the more accurate and representative bulk density values of Ryugu grains. However, there are limitations in determining the range of bulk density of individual Ryugu grains in our work due to a relatively large uncertainty in the volume estimation. The next step is to obtain more accurate individual-density data. Finally, we installed a micro-CT imaging system at our facility in February 2023. Utilizing micro-CT will provide further accurate analyses not only of the bulk density, but also of the porosity of Ryugu grains. Furthermore, micro-CT imaging enables more precise size measurements and detailed shape analyses of grains. Although the number of examined grains may be limited by CT imaging, together with the data provided in this study will help to understand the density and other physical properties of the Ryugu samples, this will provide clues regarding the generation of Ryugu grains and the evolutionary history of Ryugu.

Appendix
A1: Examination of correction factors

A newly calibrated correction factor was determined among following four candidates; (1) $k = 0.860$, by the arithmetic mean of individual k of 15 grains (used in this study), (2) $k\_wa = 0.849$, weighted mean, (3) $k\_is = 0.930$, by the least-squares approximation, and 4) $k\_ls = 0.853$, by the least-squares approximation (calculated without C0002). V_g of 15 grains were calculated using each k candidate value from Eq. (1) and compared to V_{XCT}. Figure 10 shows good correlation between V_g and V_{XCT} especially for small grains were found for three candidates of
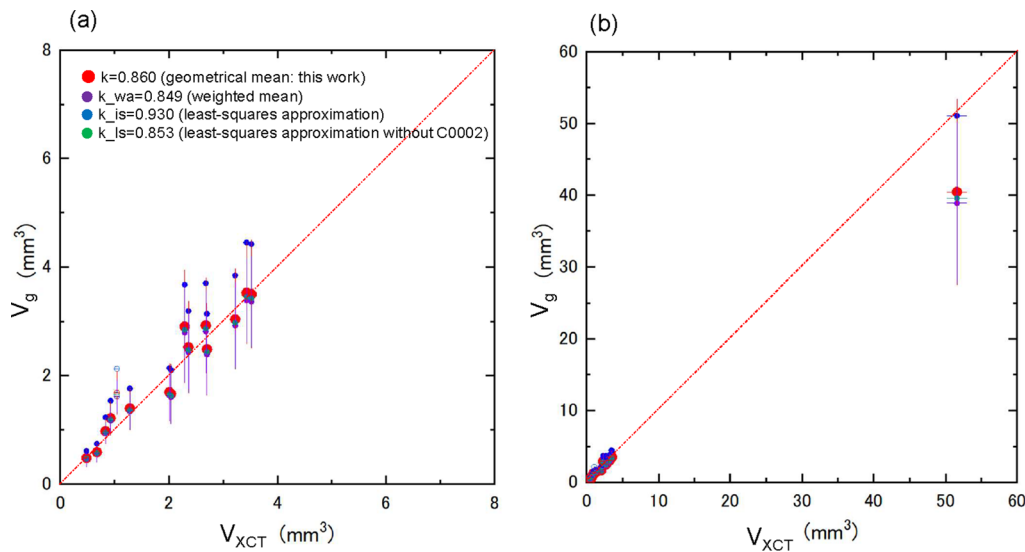
Fig. 10 Correlation between V_{XCT} and V_g calculated using four candidate k values. V_g were calculated using various *k* values: *k* = 0.860 (the geometrical mean of 15 grains, adopted value in this study); *k_wa* = 0.849 (weighted mean); *k_is* = 0.930 (the least-squares approximation); *k_ls* = 0.853 (the least-squares approximation, without C0002) from Eq. (1). **a** is an enlarged plot of a part of **b**

Table 4 Comparison between V_{XCT} and V_g calculated based on various *k* values

	K^a 0.860	k_wa^b 0.849	k_is^c 0.930	k_ls^d 0.853
V_{XCT} of 15 grains (mm³)ᵉ	80.0 ± 1.4			
V_g of 15 grains (mm³)ᵉ	69.4 ± 13.2	66.7 ± 11.4	87.6 ± 14.8	67.9 ± 11.6

[a] Geometrical mean of 15 grains, adopted in this work

[b] Weighted mean of 15 grains

[c] Least-squares approximation of 15 grains

[d] Least-squares approximation of 14 grains without C0002

[e] Obtained volume with 1σ variation

k, *k_wa* and *k_ls* but *k_is*. Among the three candidates of *k*, *k_wa* and *k_ls*, sum of V_g, 69.38 ± 13.20 mm³, calculated applying *k*, was the closest value to sum of V_{XCT}, 80.04 ± 1.40 mm³ (Table 4). The large uncertainty in for the C0002 grain was due to the uncertainty of the thickness measurement derived from a relatively large depth of field (see text).

A2: Results of KS test
See Tables 5, 6.

Table 5 Results from one-sample Kolmogorov–Smirnov test

	Bulk density	b_f/a_f	t/a_f
A			
Average valueᵃ	1.81 ± 0.30	0.70 ± 0.11	0.60 ± 0.14
KS statistic	0.058	0.043	0.058
p-value	0.14	0.42	0.13
C			
Average valueᵃ	1.76 ± 0.33	0.68 ± 0.11	0.56 ± 0.14
KS statistic	0.075	0.045	0.056
p-value	0.12	0.57	0.30

[a] Obtained value with 1σ variation

Table 6 Results from two-sample Kolmogorov–Smirnov test

	Bulk density A vs.C	b_f/a_f A vs. C	t/a_f	b_f/a_f Returned sample vs. Flying particles	t/a_f
KS statistic	0.114	0.093	0.171	0.251	0.260
p-value	0.04	0.09	0.00	0.00	0.00

Miyazaki et al. Earth, Planets and Space (2023) 75:171

Page 16 of 18

Abbreviations

CAM-H	Small monitor camera head of Hayabusa2 spacecraft
CC	Clean chamber
FE-SEM–EDS	A field emission-scanning electron microscopy/energy dispersive X-ray spectroscopy
KS test	Kolmogorov–Smirnov (static) test
JAXA	Japan Aerospace Exploration Agency
MARA	MASCOT radiometer
MASCOT	Mobile Asteroid Surface Scout
MicrOmega	Near-infrared hyperspectral microscope
SCI	Small Carry-on Impactor
TD1	First touch-down operation
TD2	Second touch-down operation
TIR	Thermal Infrared Imager
XCT	X-ray micro-computed tomography

Author contributions
AM conducted sample processing, data acquisition and wrote the paper with input from all coauthors. TY conducted sample processing, data acquisition and contributed to processed data discussions. KY, KH, AN, KN, KK, YH and RK conducted sample processing, data acquisition and summarized the data for manuscript preparation. RT conducted data acquisition and contributed to proof the manuscript. MN, HS, AN, MY, AI and SF contributed to sample image processing and data management and contributed to instrumental and environmental preparation for sample analysis. AT contributed to establishing the particle volume and density estimation method and with TM to processed data discussions. MA, TO, TU and ST supervised the research. All authors contributed to the data interpretation, commented and approved the manuscript.

Availability of data and materials
All images and data used in this study are available at the JAXA Data Archives and Transmission System (DARTS) at "Hayabusa2, Ryugu Sample Curatorial Dataset" (https://doi.org/10.17597/ISAS.DARTS/CUR-Ryugu-description). The analyzed datasets are available in the repository, as Extended Data Table S1, https://data.darts.isas.jaxa.jp/pub/curation/paper/Miyazaki_2023/.

Declarations

Competing interests
The authors declare that they have no competing interests.

Author details
[1]Institute of Space and Astronautical Science (ISAS), Japan Aerospace Exploration Agency (JAXA), Sagamihara, Kanagawa 252-5210, Japan. [2]Marine Works Japan Ltd., Yokosuka 237-0063, Japan. [3]National Institute of Polar Research (NIPR), Tachikawa, Tokyo 190-8581, Japan. [4]Ritsumeikan University, Kusatsu 525-8577, Japan. [5]CAS Key Laboratory of Mineralogy and Metallogeny/Guangdong Provincial Key Laboratory of Mineral Physics and Materials, Guangzhou Institute of Geochemistry, Chinese Academy of Science (CAS), Guangzhou 51640, People's Republic of China. [6]CAS Center for Excellence in Deep Earth Science, Guangzhou 51640, People's Republic of China. [7]Department of Earth and Planetary Science, The University of Tokyo, Bunkyo, Tokyo 113-0033, Japan. [8]Faculty of Engineering, Kindai University, Higashi-Hiroshima 739-2116, Japan. [9]The Graduate University for Advanced Studies (SOKENDAI), Hayama, 240-0193, Japan. [10]The University of Tokyo, Bunkyo, Tokyo 113-0033, Japan.

References
Bagheri GH, Bonadonna C, Manzella I, Vonlanthen P (2015) On the characterization of size and shape of irregular particles. Powder Technol 270:141–153. https://doi.org/10.1016/j.powtec.2014.10.015

Blott SJ, Pye K (2008) Particle shape: a review and new methods of characterization and classification. Sedimentology 55:31–63. https://doi.org/10.1111/j.1365-3091.2007.00892.x

Britt DT, Consolmagno GJ (2000) The porosity of dark meteorites and structure of low-albedo asteroids. Icarus 146:213–219. https://doi.org/10.1006/icar.2000.6374

Consolmagno GJ, Britt DT (1998) The density and porosity of meteorites from the Vatican collection. Meteorit Planet Sci 33:1231–1241. https://doi.org/10.1111/j.1945-5100.1998.tb01308.x

Corrigan CM, Zolensky ME, Dahl J, Long M, Weir J, Sapp C, Burkett PJ (1997) The porosity and permeability of chondritic meteorites and interplanetary dust particles. Meteorit Planet Sci 32:509–515. https://doi.org/10.1111/j.1945-5100.1997.tb01296.x

Flynn GJ, Consolmagno GJ, Brown P, Macke RJ (2018) Physical properties of the stone meteorites: implications for the properties their parent bodies. Geochemistry 78:269–298. https://doi.org/10.1016/j.chemer.2017.04.002

Gounelle M, Zolensky ME (2001) A terrestrial origin for sulfate veins in CI1 chondrites. Meteorit Planet Sci 36:1321–1329. https://doi.org/10.1111/j.1945-5100.2001.tb01827.x

Grott M, Knollenberg J, Hamm M, Ogawa K, Jaumann R, Otto KA, Delbo M, Michel P, Biele J, Neumann W, Knapmeyer M, Kührt E, Senshu H, Okada T, Helbert J, Maturilli A, Müller N, Hagermann A, Sakatani N, Tanaka S, Arai T, Mottola S, Tachibana S, Pelivan I, Drube L, Vincen J, Yano H, Pilorget C, Matz KD, Schmitz N, Koncz A, Schröder SE, Trauthan F, Schlotterer M, Krause C, Ho T, Moussi-Soffys A (2019) Low thermal conductivity boulder with high porosity identified on C-type asteroid (162173) Ryugu. Nat Astron 3:971–976. https://doi.org/10.1038/s41550-019-0832-x

Hildebrand AR, McCausland PJA, Brown PG, Longstaffe FJ, Russell SDJ, Tagliaferri E, Wacker JF, Mazur MJ (2006) The fall and recovery of the Tagish Lake meteorite. Meteorit Planet Sci 41:407–431. https://doi.org/10.1111/j.1945-5100.2006.tb00471.x

Ito M, Tomioka N, Uesugi M, Yamaguchi A, Shirai N, Ohigashi T, Liu MC, Greenwood RC, Kimura M, Imae N, Uesugi K, Nakato A, Yogata K, Yuzawa H, Kodama Y, Tsuchiyama A, Yasutake M, Findlay R, Franchi IA, Malley JA, McCain KA, Matsuda N, McKeegan KD, Hirahara K, Takeuchi A, Sekimoto S, Sakurai I, Okada I, Karouji Y, Arakawa M, Fujii A, Fujimoto M, Hayakawa M, Hirata N, Hirata N, Honda R, Honda C, Hosoda S, Iijima Y, Ikeda H, Ishiguro M, Ishihara Y, Iwata T, Kawahara K, Kikuchi S, Kitazato K, Matsumoto K, Matsuoka M, Michikami T, Mimasu Y, Miura A, Mori O, Morota T, Nakazawa S, Namiki N, Noda H, Noguchi R, Ogawa N, Ogawa K, Okada T, Okamoto C, Ono G, Ozaki M, Saiki T, Sakatani N, Sawada H, Senshu H, Shimaki Y, Shirai K, Sugita S, Takei Y, Takeuchi H, Tanaka S, Tatsumi E, Terui F, Tsukizaki R, Wada K, Yamada M, Yamada T, Yamamoto Y, Yano H, Yokota Y, Yoshihara K, Yoshikawa M, Yoshikawa K, Fukai R, Furuya S, Hatakeda K, Hayashi T, Hitomi Y, Kumagai K, Miyazaki A, Nishimura M, Soejima H, Iwamae A, Yamamoto D, Yoshitake M, Yada T, Abe M, Usui T, Watanabe S, Tsuda Y (2022) A pristine record of outer Solar System materials from asteroid Ryugu's returned sample. Nat Astron 6:1163–1171. https://doi.org/10.1038/s41550-022-01745-5

Loizeau D, Pilorget C, Riu L, Brunetto R, Bibring JP, Nakato A, Aléon-Toppani A, Hatakeda K, Yogata K, Carter J, Le Pivert-Jolivet T, Yada T, Okada T, Ususi T, Langevin Y, Lantz C, Baklouti D, Miyazaki A, Nishimura M, Nagashima K, Kumagai K, Hitomi Y, Abe M, Saiki T, Tanaka S, Nakazawa S, Tsuda Y, Watanabe S (2023) Constraints on solar system early evolution by MicrOmega analysis of Ryugu carbonate. Nat Astron 7:391–397. https://doi.org/10.1038/s41550-022-01870-1

Miyazaki *et al. Earth, Planets and Space*   (2023) 75:171

Page 17 of 18

Macke RJ, Consolmagno GJ, Britt DT (2011) Density, porosity, and magnetic susceptibility of carbonaceous chondrites. Meteorit Planet Sci 46:1842–1862. https://doi.org/10.1111/j.1945-5100.2011.01298.x

Michikami T, Honda C, Miyamoto H, Hirabayashi M, Hagermann A, Irie T, Nomura K, Ernst CM, Kawamura M, Sugimoto K, Tatsumi E, Morota T, Hirata N, Noguchi T, Cho Y, Kameda S, Kouyama T, Yokota Y, Noguchi R, Hayakawa M, Hirata N, Honda R, Matsuoka M, Sakatani N, Suzuki H, Yamada M, Yoshioka K, Sawada H, Hemmi R, Kikuchi H, Ogawa K, Watanabe S, Tanaka S, Yoshikawa M, Tsuda Y, Sugita S (2019) Boulder size and shape distributions on asteroid Ryugu. Icarus 331:179–191. https://doi.org/10.1016/j.icarus.2019.05.019

Mindat.org. (2023) Open database of minerals, rocks, meteorites and the localities. https://www.mindat.org. Accessed 25 June 2023.

Nakamura E, Kobayashi K, Tanaka R, Kunihiro T, Kitagawa H, Potiszil C, Ota T, Sakaguchi C, Yamanaka M, Ratnayake DM, Tripathi H, Kumar R, Avramescu M-L, Tsuchida H, Yachi Y, Miura H, Abe M, Fukai R, Furuya S, Hatakeda K, Hayashi T, Hitomi Y, Kumagai K, Miyazaki A, Nakato A, Nishimura M, Okada T, Soejima H, Sugita S, Suzuki A, Usui T, Yada T, Yamamoto D, Yogata K, Yoshitake M, Arakawa M, Fujii A, Hayakawa M, Hirata N, Hirata N, Honda R, Honda C, Hosoda S, Iijima Y, Ikeda H, Ishiguro M, Ishihara Y, Iwata T, Kawahara K, Kikuchi S, Kitazato K, Matsumoto K, Matsuoka M, Michikami T, Mimasu Y, Miura A, Morota T, Nakazawa S, Namiki N, Noda H, Noguchi R, Ogawa N, Ogawa K, Okamoto C, Ono G, Ozaki M, Saiki T, Sakatani N, Sawada H, Senshu H, Shimaki Y, Shirai K, Takei Y, Takeuchi H, Tanaka S, Tatsumi E, Terui F, Tsukizaki R, Wada K, Yamada M, Yamada T, Yamamoto Y, Yano H, Yokota Y, Yoshihara K, Yoshikawa M, Yoshikawa K, Fujimoto M, Watanabe S, Tsuda Y (2022a) On the origin and evolution of the asteroid Ryugu: A comprehensive geochemical perspective. Proc Jpn Acad Ser B98:227–282. https://doi.org/10.2183/pjab.98.015

Nakamura T, Matsumoto M, Amano K, Enokido Y, Zolensky ME, Mikouchi T, Genda H, Tanaka S, Zolotov MY, Kurosawa K, Wakita S, Hyoudo R, Nagano H, Nakashima D, Takahashi Y, Fujioka Y, Kikuiri M, Kagawa E, Matsuoka M, Brealey AJ, Tsuchiyama A, Uesugi M, Matsuno J, Kimura Y, Sato M, Milliken RE, Tatsumi E, Sugita S, Hiroi T, Kitazono K, Brownlee D, Joswiak DJ, Takahashi M, Ninomiya K, Osawa T, Terada K, Brenker FE, Tkalcec BJ, Vincze L, Brunetto R, Aleon-Toppani A, Chan QHS, Roskosz M, Vinnet J-C, Beck P, Alp EE, Michikami T, Nagaashi Y, Tsuji T, Ino Y, Martinez J, Han J, Dolocan A, Bodnar RJ, Tanaka M, Yoshida H, Sugiyama K, King AJ, Fukushi K, Suga H, Yamashita S, Kawai T, Inoue K, Nakato A, Noguchi T, Vilas F, Hendrix AR, Jaramillo-Correa C, Domingue DL, Dominguez G, Gainsforth Z, Engrand C, Duprat J, Russell SS, Bonato E, Ma C, Kawamoto T, Wada T, Watanabe S, Endo R, Enju S, Riu L, Rubino S, Tack P, Takeshita S, Takeichi Y, Takeuchi A, Takigawa A, Takir D, Tanigaki T, Taniguchi A, Tsukamoto K, Yagi T, Yamada S, Yamamoto K, Yamashita Y, Yasutake M, Uesugi K, Umegaki I, Chiu I, Ishizaki T, Okumura S, Palomba E, Pilorget C, Potin SM, Alasli A, Anada S, Araki Y, Sakatani N, Schulz C, Sekizawa O, Sitzman SD, Sugiura K, Sun M, Dartois E, De Pauw E, Dionnet Z, Djouadi Z, Falkenberg G, Fujita R, Fukuma T, Gearba IR, Hagiya K, Hu MY, Kato T, Kawamura T, Kimura M, Kubo MK, Langenhorst F, Lantz C, Lavina B, Lindner M, Zhao J, Vekemans B, Baklouti D, Bazi B, Borondics F, Nagasawa S, Nishiyama G, Nitta K, Mathurin J, Matsumoto T, Mitsukawa I, Miura H, Miyake A, Miyake Y, Yurimoto H, Okazaki R, Yabuta H, Naraoka H, Sakamoto K, Tachibana S, Connolly HC Jr, Lauretta DS, Yoshitake M, Yoshikawa M, Yoshikawa K, Yoshihara K, Yokota Y, Yogata K, Yano H, Yamamoto Y, Yamamoto D, Yamada M, Yamada T, Yada T, Wada K, Usui T, Tsukizaki R, Terui F, Takeuchi H, Takei Y, Iwamae A, Soejima H, Shirai K, Shimaki Y, Senshu H, Sawada H, Saiki T, Ozaki M, Ono G, Okadda T, Ogawa N, Ogawa K, Noguchi R, Noda H, Nishimura M, Namiki N, Nakazawa S, Morota T, Miyazaki A, Miura A, Mimasu Y, Matsumoto K, Kumagai K, Kouyama T, Kikuchi S, Kawahara K, Kameda S, Iwata T, Ishihara Y, Ishiguro M, Ikeda H, Hosoda S, Honda R, Honda C, Hitomi Y, Hirata N, Hayashi T, Hayakawa M, Hatakeda K, Furuya S, Fukai R, Fujii A, Cho Y, Arakawa M, Abe M, Watanabe S, Tsuda Y (2022b) Formation and evolution of carbonaceous asteroid Ryugu: direct evidence from returned samples. Science 379:eabn8671. https://doi.org/10.1126/science.abn8671

Nakato A, Yada T, Nishimura M, Yogata K, Miyazaki A, Nagashima K, Hatakeda K, Kumagai K, Hitomi Y, Soejima H, Bibring JP, Pilorget C, Hamm V, Brunetto R, Riu L, Lourit L, Loizeau D, Le Pivert-Jolivet T, Lequertier G, Moussi-Soffys A, Abe M, Okada T, Usui T, Nakazawa S, Saiki T, Tanaka S, Terui F, Yoshikawa M, Watanabe S, Tsuda Y (2023) Variations of the surface characteristics of Ryugu returned samples. Earth Planets Space 75:45. https://doi.org/10.1186/s40623-022-01754-8

Naraoka H, Takano Y, Dworkin JP, Oba Y, Hamase K, Furusho A, Ogawa NO, Hashiguchi M, Fukushima K, Aoki D, Schmitt-Kopplin P, Aponte JC, Parker ET, Glavin DP, McLain HL, Elsila JE, Graham HV, Eiler JM, Orthous-Daunay FR, Wolters C, Isa J, Vuitton V, Thissen R, Sakai S, Yoshimura T, Koga T, Ohkouchi N, Chikaraishi Y, Sugahara H, Mita H, Furukawa Y, Hertkorn N, Ruf A, Yurimoto H, Nakamura T, Noguchi T, Okazaki R, Yabuta H, Sakamoto K, Tachibana S, Harold C, Connolly HC Jr, Lauretta DS, Abe M, Yada T, Nishimura M, Yogata K, Nakato A, Yoshitake M, Suzuki A, Miyazaki A, Furuya S, Hatakeda K, Soejima H, Hitomi Y, Kumagai K, Usui T, Hayashi T, Yamamoto D, Fukai R, Kitazato K, Sugita S, Noriyuki Namiki N, Arakawa M, Ikeda H, Ishiguro M, Hirata N, Wada K, Ishihara Y, Noguchi R, Morota T, Sakatani N, Matsumoto K, Senshu H, Honda R, Tatsumi E, Yokota Y, Honda C, Michikami T, Matsuoka M, Miura A, Noda H, Yamada T, Yoshihara K, Kawahara K, Ozaki M, Iijima Y, Yano H, Hayakawa M, Iwata T, Tsukizaki R, Sawada H, Hosoda S, Ogawa K, Okamoto C, Hirata N, Shirai K, Shimaki Y, Yamada M, Okada T, Yamamoto Y, Takeuchi H, Fujii A, Takei Y, Yoshikawa K, Mimasu Y, Ono G, Ogawa N, Kikuchi S, Nakazawa S, Terui F, Tanaka S, Saiki T, Yoshikawa M, Watanabe S, Tsuda Y (2023) Soluble organic molecules in samples of the carbonaceous asteroid (162173) Ryugu. Science 379:eabn9033. https://doi.org/10.1126/science.abn9033

Nishimura M, Nakato A, Abe M, Nagashima K, Soejima H, Yada T, Yogata K, MiyazakiA HK, Yoshitake M, Iwamae A, Pilorget C, Brunetto R, Loizeau D, Bibring JP, Riu L, Yumoto K, Cho Y, Yabe Y, Sugita S, Ito M, Okada T, Tachibana S, Usui T (2023) Ryugu Sample Database System (RS-DBS) on the Data Archives and Transmission System (DARTS) by the JAXA curation. Earth Planets Space. https://doi.org/10.1186/s40623-023-01887-4

Noguchi T, Matsumoto T, Miyake A, Igami Y, Haruta M, Saito H, Hata S, Seto Y, Miyahara M, Tomioka N, Ishii HA, Bradley JP, Ohtaki K, Dobrică E, Leroux H, Guillou CL, Jacob D, Peña F, Laforet S, Marinova M, Langenhorst F, Harries D, Beck P, Phan THV, Rebois R, Abreu NM, Gray J, Zega T, Zanetta PM, Thompson MS, Stroud R, Burgess K, Cymes BA, Bridges JC, Hicks L, Lee MR, Daly L, Bland PA, Zolensky ME, Frank DR, Martinez J, Tsuchiyama A, Yasutake M, Matsuno J, Okumura S, Mitsukawa I, Uesugi K, Uesugi M, Takeuchi A, Sun M, Enju S, Takigawa A, Michikami T, Nakamura T, Matsumoto M, Nakauchi Y, Abe M, Arakawa M, Fujii A, Hayakawa M, Hirata N, Hirata N, Honda R, Honda C, Hosoda S, Iijima Y, Ikeda H, Ishiguro M, Ishihara Y, Iwata T, Kawahara K, Kikuchi S, Kitazato K, Matsumoto K, Matsuoka M, Mimasu Y, Miura A, Morota T, Nakazawa S, Noriyuki Namiki N, Noda H, Noguchi R, Ogawa N, Ogawa K, Okada T, Okamoto C, Ono G, Ozaki M, Saiki T, Sakatani N, Sawada H, Senshu H, Shimaki Y, Shirai K, Sugita S, Takei Y, Takeuchi H, Tanaka S, Tatsumi E, Terui F, Tsukizaki R, Wada K, Yamada M, Yamada T, Yamamoto Y, Yano H, Yokota Y, Yoshihara K, Yoshikawa M, Yoshikawa K, Fukai R, Furuya S, Hatakeda K, Hayashi T, Hitomi Y, Kumagai K, Miyazaki A, Nakato A, Nishimura M, Soejima H, Iwamae A, Usui T, Yada T, Yamamoto D, Yogata K, Yoshitake M, Connolly HC Jr, Lauretta DS, Yurimoto H, Nagashima K, Kawasaki N, Sakamoto N, Okazaki R, Yabuta H, Naraoka H, Sakamoto K, Tachibana S, Watanabe S, Tsuda Y (2023) A dehydrated space-weathered skin cloaking the hydrated interior of Ryugu. Nat Astron 7:170–181. https://doi.org/10.1038/s41550-022-01841-6

Okada T, Fukuhara T, Tanaka S, Taguchi M, Arai T, Senshu H, Sakatani N, Shimaki Y, Demura H, Ogawa Y, Suko K, Sekiguchi T, Kouyama T, Takita J, Matsunaga T, Imamura T, Wada T, Hasegawa S, Helbert J, Müller T, Hagermann A, Biele J, Hamm M, Delbo M, Hirata N, Hirata N, Yamamoto Y, Sugita S, Namiki N, Kitazono K, Arakawa M, Tachibana S, Ikeda H, Ichiguro M, Wada K, Honda C, Ishihara Y, Matsumoto K, Matsuoka M, Micchikami T, Miura A, Morota T, Noda H, Noguchi R, Ogawa K, Shirai K, Tatsumi E, Yabuta H, Yokoda Y, Yamada M, Abe M, Hayakawa M, Iwata T, Ozaki M, Yano H, Hosoda S, Mori O, Sawada H, Shimada T, Takeuchi HH, Tsukizaki R, Fujii A, Hirose C, Kikuchi S, Mimasu Y, Ogawa N, Ono G, Takahashi T, Takei Y, Yamaguchi T, Yoshikawa K, Terui F, Saiki T, Nakazawa S, Yoshikawa M, Watanabe S, Tsuda Y (2019) Highly porous nature of a primitive asteroid revealed by thermal imaging. Nature 579:518–525. https://doi.org/10.1038/s41586-020-2102-6

Okazaki R, Marty B, Busemann H, Hashizume K, Gilmour JD, Meshik A, Yada T, Kitajima F, Broadley MW, Byrne D, Füri E, Riebe MEI, Krietsch D, Maden C, Ishida A, Clay P, Crowther SA, Fawcett L, Lawton T, Pravdivtseva O, Miura YN, Park J, Bajo K, Takano Y, Yamada K, Kawagucci S, Matsui Y, Yamamoto M, Righter K, Sakai S, Iwata N, Shirai N, Sekimoto S, Inagaki M, Ebihara M, Yokochi R, Nishiizumi K, Nagao K, Lee JIK, Kano A, Caffee MW, Uemura R, Nakamura T, Naraoka H, Noguchi T, Yabuta H, Yurimoto H, Tachibana S, Sawada H, Sakamoto K, Abe M, Arakawa M, Fujii A, Hayakawa M, Hirata N, Hirata N, Honda R, Honda C, Hosoda S, Iijima Y, Ikeda H, Ishiguro M, Ishihara Y, Iwata T, Kawahara K, Kikuchi

Miyazaki *et al. Earth, Planets and Space*   (2023) 75:171

Page 18 of 18

S, Kitazato K, Matsumoto K, Matsuoka M, Michikami T, Mimasu Y, Miura A, Morota T, Nakazawa S, Namiki N, Noda H, Noguchi R, Ogawa N, Ogawa K, Okada T, Okamoto C, Ono G, Ozaki M, Saiki T, Sakatani N, Senshu H, Shimaki Y, Shirai K, Sugita S, Takei Y, Takeuchi H, Tanaka S, Tatsumi E, Terui F, Tsukizaki R, Wada K, Yamada M, Yamada T, Yamamoto Y, Yano H, Yokota Y, Yoshihara K, Yoshikawa M, Yoshikawa K, Furuya S, Hatakeda K, Hayashi T, Hitomi Y, Kumagai K, Miyazaki A, Nakato A, Nishimura M, Soejima H, Iwamae A, Yamamoto D, Yogata K, Yoshitake M, Fukai R, Usui T, Connolly HC Jr, Lauretta D, Watanabe S, Yuichi Tsuda Y (2022) Noble gases and nitrogen in samples of asteroid Ryugu record its volatile sources and recent surface evolution. Science 379:eabo0431. https://doi.org/10.1126/science.abo0431

Pilorget C, Okada T, Hamm V, Brunetto R, Yada T, Loizeau D, Riu L, Usui T, Moussi-Soffys A, Hatakeda K, Nakato A, Yogata K, Abe M, Aléon-Toppani A, Carter J, Chaigneau M, Crane B, Gondet B, Kumagai K, Langevin Y, Lantz C, Le Pivert-Jolivet T, Lequertier G, Lourit L, Miyazaki A, Nishimura M, Poulet F, Arakawa M, Hirata N, Kitazato K, Nakazawa S, Namiki N, Saiki T, Sugita S, Tachibana S, Tanaka S, Yoshikawa M, Tsuda Y, Watanabe S, Bibring JP (2022) First compositional analysis of Ryugu samples by the MicrOmega hyperspectral microscope. Nat Astron 6:221–225. https://doi.org/10.1038/s41550-021-01549-z

Sawada H, Okazaki R, Tachibana S, Sakamoto K, Takano Y, Okamoto C, Yano H, Miura Y, Abe M, Hasegawa S, Noguchi T (2017) Hayabusa2 Sampler: Collection of asteroidal surface material. Space Sci Rev 208:1. https://doi.org/10.1007/s11214-017-0338-8

Tachibana S, Sawada H, Okazaki R, Takano Y, Sakamoto K, Miura YN, Okamoto C, Yano H, Yamanouchi S, Michel P, Zhang Y, Schwartz S, Thuillet F, Yurimoto H, Nakamura T, Noguchi T, Yabuta H, Naraoka H, Tsuchiyama A, Imae N, Kurosawa K, Nakamura AM, Ogawa K, Sugita S, Morota T, Honda R, Kameda S, Tatsumi E, Cho Y, Yoshioka K, Yokota Y, Hayakawa M, Matsuoka M, Sakatani N, Yamada M, Kouyama T, Suzuki H, Honda C, Yoshimitsu T, Kubota T, Demura H, Yada T, Nishimura M, Yogata K, Nakato A, Yoshitake M, Suzuki AI, Furuya S, Hatakeda K, Miyazaki A, Kumagai K, Okada T, Abe M, Usui T, Ireland TR, Fujimoto M, Yamada T, Arakawa M, Connolly HC Jr, Fujii A, Hasegawa S, Hirata N, Hirata N, Hirose C, Hosoda S, Iijima Y, Ikeda H, Ishiguro M, Ishihara Y, Iwata T, Kikuchi S, Kitazato K, Lauretta DS, Libourel G, Marty B, Matsumoto K, Michikami T, Mimasu Y, Miura A, Mori O, Nakamura-Messenger K, Namiki N, Nguyen AN, Nittler LR, Noda H, Noguchi R, Ogawa N, Ono G, Ozaki M, Senshu H, Shimada T, Shimaki T, Shirai K, Soldini S, Takahashi T, Takei Y, Takeuchi H, Tsukizaki R, Wada K, Yamamoto Y, Yoshikawa K, Yumoto K, Zolensky ME, Nakazawa S, Terui F, Tanaka S, Saiki T, Yoshikawa M, Watanabe S, Tsuda Y (2022) Pebbles and sands on asteroid (162173) Ryugu: on-site observation and returned particles from two landing sites. Science 375:1011–1016. https://doi.org/10.1126/science.abj8624

Yabuta H, Cody GD, Engrand C, Kebukawa Y, Gregorio BD, Bonal L, Remusat L, Stroud R, Quirico E, Nittler L, Hashiguchi M, Komatsu M, Okumura T, Mathurin J, Dartois E, Duprat J, Takahashi Y, Takeichi Y, Kilcoyne D, Yamashita S, Dazzi A, Deniset-Besseau A, Sandford S, Martins Z, Tamenori Y, Ohigashi T, Suga H, Wakabayashi D, Verdier-Paoletti M, Mostefaoui S, Montagnac G, Barosch J, Kamide K, Shigenaka M, Bejach L, Matsumoto M, Enokido Y, Noguchi T, Yurimoto H, Nakamura T, Okazaki R, Naraoka H, Sakamoto K, Connolly HCJR, Lauretta DS, Abe M, Okada T, Yada T, Nishimura M, Yogata K, Nakato A, Yoshitake M, Iwamae A, Furuya S, Hatakeda K, Miyazaki A, Soejima H, Hitomi Y, Kumagai K, Usui T, Hayashi T, Yamamoto D, Fukai R, Sugita S, Kitazato K, Hirata N, Honda R, Morota T, Tatsumi E, Sakatani N, Namiki N, Matsumoto K, Noguchi R, Wada K, Senshu H, Ogawa K, Yokota Y, Ishihara Y, Shimaki Y, Yamada M, Honda C, Michikami T, Matsuoka M, Hirata N, Arakawa M, Okamoto C, Ishiguro M, Jaumann R, Bibring J, Grott M, Schröder S, Otto K, Pilorget C, Schmitz N, Biele J, Ho T, Moussi-Soffys A, Miura A, Noda H, Yamada T, Yoshihara K, Kawahara K, Ikeda H, Yamamoto Y, Shirai K, Kikuchi S, Ogawa N, Takeuchi H, Ono G, Mimasu Y, Yoshikawa K, Takei Y, Fujii A, Iijima Y, Nakazawa S, Hosoda S, Iwata T, Hayakawa M, Sawada H, Yano H, Tsukizaki R, Ozaki M, Terui F, Tanaka S, Fujimoto M, Yoshikawa M, Saiki T, Tachibana S, Watanabe S, Tsuda Y (2023) Macromolecular organic matter in sample of the asteroid (162173) Ryugu. Science 379:eabn9057. https://doi.org/10.1126/science.abn9057

Yada T, Abe M, Okada T, Nakato A, Yogata K, Miyazaki A, Hatakeda K, Kumagai K, Nishimura M, Hitomi Y, Soejima H, Yoshitake M, Iwamae A, Furuya S, Uesugi M, Karouji Y, Usui T, Hayashi T, Yamamoto D, Fukai R, Sugita S, Cho Y, Yumoto K, Yabe Y, Bibring J-P, Pilorget C, Hamm V, Brunetto R, Riu L, Lourit L, Loizeau D, Lequertier G, Moussi-Soffys A, Tachibana S, Sawada H, Okazaki R, Takano Y, Sakamoto K, Miura YN, Yano H, Ireland TR, Yamada M, Fujimoto M, Kitazato

K, Namiki N, Arakawa M, Hirata N, Yurimoto H, Nakamura T, Noguchi T, Yabuta H, Naraoka H, Ito M, Nakamura E, Uesugi K, Kobayashi K, Michikami T, Kikuchi H, Hirata N, Ishihara Y, Matsumoto K, Noda H, Noguchi R, Shimaki Y, Shirai K, Ogawa K, Wada K, Senshu H, Yamamoto Y, Morota T, Honda R, Honda C, Yokota Y, Matsuoka M, Sakatani N, Tatsumi E, Miura A, Yamada M, Fujii A, Hirose C, Hosoda S, Ikeda H, Iwata T, Kikuchi S, Mimasu Y, Mori O, Ogawa N, Ono G, Shimada T, Soldini S, Takahashi T, Takei Y, Takeuchi H, Tsukizaki R, Yoshikawa K, Terui F, Nakazawa S, Tanaka S, Saiki T, Yoshikawa M, Watanabe S-I, Tsuda Y (2022) Preliminary analysis of the Hayabusa2 samples returned from C-type asteroid Ryugu. Nat Astron 6:214–220. https://doi.org/10.1038/s41550-021-01550-6

Yada T, Abe M, Nishimura M, Sawada H, Okazaki R, Takano Y, Sakamoto K, Okada T, Nakato A, Yoshitake M, Nakano Y, Yogata K, Miyazaki A, Furuya S, Iwamae AS, Nakatsubo S, Hatakeda K, Hitomi Y, Kumagai K, Suzuki S, Miura YN, Ito M, Tomioka N, Uesugi M, Karouji Y, Uesugi K, Shirai N, Yamaguchi A, Imae N, Naraoka H, Yamamoto Y, Tachibana S, Yurimoto H, Usui T (2023) A curation for uncontaminated Hayabusa2-returned samples in the Extraterrestrial Curation Center of JAXA: From the beginning to present day. Earth Planets Space. https://doi.org/10.1186/s40623-023-01924-2

Yokoyama T, Nagashima K, Nakai I, Young ED, Abe Y, Aléon J, Alexander CMO'D, Amari S, Amelin Y, Bajo K, Bizzarro M, Bouvier A, Carlson RW, Chaussidon M, Choi B, Dauphas N, Davis AM, Di Rocco T, Fujiya W, Fukai R, Gautam I, Haba MK, Hibiya Y, Hidaka H, Homma H, Hoppe P, Huss GR, Ichida K, Iizuka T, Ireland TR, Ishikawa A, Ito M, Itoh S, Kawasaki N, Kita NT, Kitajima K, Kleine T, Komatani S, Krot AN, Liu M, Masuda Y, McKeegan KD, Morita M, Motomura K, Moynier F, Nguyen A, Nittler L, Onose M, Pack A, Park C, Piani L, Qin L, Russel SS, Sakamoto N, Schönbächler M, Tafla L, Tang H, Terada K, Terada Y, Usui T, Wada S, Wadhwa M, Walker RJ, Yamashita K, Yin Q, Yoneda S, Yui H, Zhang A, Connolly HC Jr, Lauretta DS, Nakamura T, Naraoka H, Noguchi T, Okazaki R, Sakamoto K, Yabuta H, Abe M, Arakawa M, Fujii A, Hayakawa M, Hirata N, Honda R, Honda C, Hosoda S, Iijima Y, Ikeda H, Ishiguro M, Ishihara Y, Iwata T, Kawahara K, Kikuchi S, Kitazato K, Matsumoto K, Matsuoka M, Michikami T, Mimasu Y, Miura A, Morota T, Nakazawa S, Namiki N, Noda H, Noguchi R, Ogawa N, Ogawa K, Okada T, Okamoto C, Ono G, Ozaki M, Saiki T, Sakatani N, Sawada H, Senshu H, Shimaki Y, Shirai K, Sugita S, TakeiY TH, Tanaka S, Tatsumi E, Terui F, Tsuda Y, Tsukizaki R, Wada K, Watanabe S, Yamada M, Yamada T, Ymamoto Y, Yano H, Yokota Y, Yoshihara K, Yoshikawa M, Yoshikawa K, Furuya S, Hatakeda K, Hayashi T, Hitomi Y, Kumagai K, Miyazaki A, Nakato A, Nishimura M, Soejima H, Suzuki A, Yada T, Yamamoto D, Yogata K, Yoshitake M, Tachibana S, Yurimoto H (2022) Samples returned from the asterioid Ryugu are similar to Ivuna-type carbonaceous meteorites. Science 379:eabn7850. https://doi.org/10.1126/science.abn7850

Zolensky ME, Nakamura K, Gounelle M, MikouchiT KT, Tachikawa O, Tonui E (2002) Mineralogy of Tagish Lake: an ungouped type 2carbonaceous chondrite. Meteorit Planet Sci 37:737–761. https://doi.org/10.1111/j.1945-5100.2002.tb00852.x

Publisher's Note

Springer Nature remains neutral with regard to jurisdictional claims in published maps and institutional affiliations.